

## The endocannabinoid *N*-arachidonoyl dopamine (NADA) selectively induces oxidative stress-mediated cell death in hepatic stellate cells but not in hepatocytes

Alexandra Wojtalla, Frank Herweck, Michaela Granzow, Sabine Klein, Jonel Trebicka, Sebastian Huss, Raissa Lerner, Beat Lutz, Frank Alexander Schildberg, Percy Alexander Knolle, Tilman Sauerbruch, Manfred Vincenz Singer, Andreas Zimmer and Sören Volker Siegmund

*Am J Physiol Gastrointest Liver Physiol* 302:G873-G887, 2012. First published 2 February 2012;  
doi: 10.1152/ajpgi.00241.2011

### You might find this additional info useful...

---

This article cites 53 articles, 11 of which you can access for free at:  
<http://ajpgi.physiology.org/content/302/8/G873.full#ref-list-1>

Updated information and services including high resolution figures, can be found at:  
<http://ajpgi.physiology.org/content/302/8/G873.full>

Additional material and information about *AJP - Gastrointestinal and Liver Physiology* can be found at:

<http://www.the-aps.org/publications/ajpgi>

---

This information is current as of September 18, 2012.

*AJP - Gastrointestinal and Liver Physiology* publishes original articles pertaining to all aspects of research involving normal or abnormal function of the gastrointestinal tract, hepatobiliary system, and pancreas. It is published 24 times a year (twice monthly) by the American Physiological Society, 9650 Rockville Pike, Bethesda MD 20814-3991. Copyright © 2012 the American Physiological Society. ISSN: 1522-1547. Visit our website at <http://www.the-aps.org/>.

## The endocannabinoid *N*-arachidonoyl dopamine (NADA) selectively induces oxidative stress-mediated cell death in hepatic stellate cells but not in hepatocytes

Alexandra Wojtalla,<sup>1,2,3</sup> Frank Herweck,<sup>3</sup> Michaela Granzow,<sup>1</sup> Sabine Klein,<sup>1</sup> Jonel Trebicka,<sup>1</sup> Sebastian Huss,<sup>4</sup> Raissa Lerner,<sup>5</sup> Beat Lutz,<sup>5</sup> Frank Alexander Schildberg,<sup>6</sup> Percy Alexander Knolle,<sup>6</sup> Tilman Sauerbruch,<sup>1</sup> Manfred Vincenz Singer,<sup>3</sup> Andreas Zimmer,<sup>2</sup> and Sören Volker Siegmund<sup>1,3</sup>

<sup>1</sup>Department of Internal Medicine I and <sup>2</sup>Institute of Molecular Psychiatry, University of Bonn, Bonn; <sup>3</sup>Department of Medicine II, University Hospital Mannheim, University of Heidelberg, Heidelberg; <sup>4</sup>Institute of Pathology, University Hospital of Cologne, Cologne; <sup>5</sup>Institute of Physiological Chemistry, University Medical Center Mainz, Mainz; and <sup>6</sup>Institutes of Molecular Medicine and Experimental Immunology, University of Bonn, Bonn, Germany

Submitted 20 June 2011; accepted in final form 1 February 2012

**Wojtalla A, Herweck F, Granzow M, Klein S, Trebicka J, Huss S, Lerner R, Lutz B, Schildberg FA, Knolle PA, Sauerbruch T, Singer MV, Zimmer A, Siegmund SV.** The endocannabinoid *N*-arachidonoyl dopamine (NADA) selectively induces oxidative stress-mediated cell death in hepatic stellate cells but not in hepatocytes. *Am J Physiol Gastrointest Liver Physiol* 302: G873–G887, 2012. First published February 2, 2012; doi:10.1152/ajpgi.00241.2011.—The endocannabinoid system is a crucial regulator of hepatic fibrogenesis. We have previously shown that the endocannabinoid anandamide (AEA) is a lipid mediator that blocks proliferation and induces death in hepatic stellate cells (HSCs), the main fibrogenic cell type in the liver, but not in hepatocytes. However, the effects of other endocannabinoids such as *N*-arachidonoyl dopamine (NADA) have not yet been investigated. The NADA-synthesizing enzyme tyrosine hydroxylase was mainly expressed in sympathetic neurons in portal tracts. Its expression pattern stayed unchanged in normal or fibrotic liver. NADA dose dependently induced cell death in culture-activated primary murine or human HSCs after 2–4 h, starting from 5  $\mu$ M. Despite caspase 3 cleavage, NADA-mediated cell death showed typical features of necrosis, including ATP depletion. Although the cannabinoid receptors CB1, CB2, or transient receptor potential cation channel subfamily V, member 1 were expressed in HSCs, their pharmacological or genetic blockade failed to inhibit NADA-mediated death, indicating a cannabinoid-receptor-independent mechanism. Interestingly, membrane cholesterol depletion with methyl- $\beta$ -cyclodextrin inhibited AEA- but not NADA-induced death. NADA significantly induced reactive oxygen species formation in HSCs. The antioxidant glutathione (GSH) significantly decreased NADA-induced cell death. Similar to AEA, primary hepatocytes were highly resistant against NADA-induced death. Resistance to NADA in hepatocytes was due to high levels of GSH, since GSH depletion significantly increased NADA-induced death. Moreover, high expression of the AEA-degrading enzyme fatty acid amide hydrolase (FAAH) in hepatocytes also conferred resistance towards NADA-induced death, since pharmacological or genetic FAAH inhibition significantly augmented hepatocyte death. Thus the selective induction of cell death in HSCs proposes NADA as a novel antifibrogenic mediator.

hepatic fibrosis

RECENTLY, IT HAS BEEN DEMONSTRATED that the endocannabinoid system, consisting of arachidonic-acid-derived endocannabinoids as ligands, their receptors, and enzymes that are respon-

sible for endocannabinoid biosynthesis and degradation, is crucially involved in the regulation of hepatic fibrogenesis. Cannabinoid receptor type 2 (CB2)<sup>-/-</sup> mice showed increased fibrogenesis in response to carbon tetrachloride (CCl<sub>4</sub>) injection, whereas CB1<sup>-/-</sup> mice displayed decreased hepatic fibrogenesis (26, 52). However, the mechanisms by which endocannabinoids regulate liver injury and fibrogenesis are not well characterized. Although it has been suggested that endocannabinoids promote the resolution of hepatic fibrosis by inducing cell death in hepatic stellate cells (HSCs), the main fibrogenic cell type in the liver, it remains elusive which endocannabinoids are involved in regulation of hepatic fibrogenesis (26, 50–52).

Endocannabinoids evoke a wide spectrum of physiological actions that are mostly mediated through the G-protein-coupled cannabinoid receptors CB1 and CB2 (15, 36) but can also occur independently of these receptors (5, 7, 26, 35, 44, 48, 50, 51). Endocannabinoids were initially described to play major roles in the central nervous system where they regulate food intake, emotions, pain perception, and sleep (16, 17, 27). More recent studies (28, 33, 39) have shown that endocannabinoids are also involved in the regulation of inflammation, cell death, and peripheral lipogenesis. *N*-arachidonoyl ethanolamide [anandamide (AEA)] and 2-arachidonoyl glycerol (2-AG) are the best characterized endocannabinoids.

Recently we and others have shown that AEA or 2-AG selectively induce cell death in HSCs (Refs. 6, 21) and therefore hold antifibrogenic properties. Interestingly, *N*-arachidonoyl dopamine (NADA), a novel endocannabinoid, also selectively induced cell death under certain circumstances in immune or neuronal cells (13, 45). NADA belongs to the endovanilloid class of endocannabinoids and was recently identified as an endogenous ligand for CB1 and transient receptor potential cation channel subfamily V, member 1 (TRPV1; Refs. 6, 24). It also shows low affinity to CB2 receptors (6, 16). In the central nervous system, NADA can be found predominantly in the striatum, hippocampus, cerebellum, and dorsal root ganglia and is proposed to play a role in neuronal pain and inflammation (23). In peripheral organs such as isolated bronchi or urinary bladder of the guinea pig, NADA showed constrictory effects mediated by TRPV1 signaling (20). In contrast, NADA initiated vasorelaxant effects also via the activation of TRPV1 and CB1 receptors in small mesenteric vessels, superior mesenteric artery (37), or aorta in rats

Address for reprint requests and other correspondence: S. V. Siegmund, Dept. of Internal Medicine I, Univ. of Bonn, Sigmund-Freud-Str. 25, D-53105 Bonn, Germany (e-mail: soeren.siegmund@ukb.uni-bonn.de).

(38). Moreover, NADA induced cell death in a human neuroblastoma cell line or in human peripheral blood mononuclear cells via TRPV1 activation (13, 45). However, the effect of NADA as a representative of this novel endovanilloid class of endocannabinoids on different liver cell populations and its function in acute or chronic liver diseases have not been elucidated so far.

In this study, we found a specific expression of the rate-limiting NADA-generating enzyme tyrosine hydroxylase (TH) mainly in sympathetic neurons in portal tracts. The expression remained constant in normal or fibrotic liver. Possibly due to a volatile nature and faster degradation in contrast to AEA, NADA was only detectable in the striatum but not in normal or fibrotic liver tissue. NADA selectively induced reactive oxygen species (ROS)-dependent necrotic cell death in primary culture- and in vivo-activated HSCs independently from cannabinoid receptors, whereas primary hepatocytes were resistant against NADA due to high expression of the endocannabinoid-degrading enzyme fatty acid amide hydrolase (FAAH) and high levels of antioxidants. Here, we show for the first time that the selective induction of cell death by NADA in HSCs but not in hepatocytes implies a possible role for this novel endocannabinoid as an antifibrotic agent.

## MATERIALS AND METHODS

**HSC, Kupffer cell, liver sinusoidal endothelial cell, and hepatocyte isolation and culture.** Primary HSCs were isolated by a two-step pronase-collagenase perfusion from the livers of male Sprague-Dawley rats (300–450 g;  $n = 20$ ), from male Sprague-Dawley rats after 21 days of bile duct ligation (BDL) or sham operation (350–400 g;  $n = 3$  each), or from C57BL/6J wild-type (25–30 g;  $n = 32$ ) or CB1<sup>-/-</sup>CB2<sup>-/-</sup> double knockout mice (25–30 g, pure C57BL/6J background;  $n = 3$ ) followed by Nycodenz (Axis-Shield, Oslo, Norway) two-layer discontinuous density gradient centrifugation as previously described (48, 50, 51). The purity of HSC preparations was 94%, as assessed by autofluorescence at day 2 after isolation. HSCs were cultured on uncoated plastic tissue culture dishes as described previously. Rat and mouse HSCs were not passaged and were considered culture-activated between day 7 and 14 after isolation. Human primary culture activated HSCs were purchased from ScienCell Research Laboratories (Carlsbad, CA), cultured as previously described (51) and used between passages 1 to 5.

To isolate Kupffer cells from healthy C57BL/6J wild-type mouse livers ( $n = 3$ ), we performed collagenase-pronase perfusion followed by 15% Nycodenz gradient centrifugation and subsequent positive selection of F4/80-expressing cells by magnetic antibody cell sorting (Miltenyi Biotec, Bergisch Gladbach, Germany; Ref. 47). Liver sinusoidal endothelial cells (LSECs) were isolated from healthy C57BL/6J wild-type mouse livers ( $n = 3$ ) after collagenase perfusion and 30% Nycodenz gradient centrifugation followed by magnetic antibody cell sorting using  $\alpha$ CD146-beads (Miltenyi Biotec; Ref. 46). Murine Kupffer cells and LSECs were not passaged and were cultured in DMEM containing 10% FBS.

Primary hepatocytes were isolated from male Sprague-Dawley rats (225–250 g;  $n = 15$ ) or from wild-type C57BL/6J mice (25–30 g, littermates;  $n = 3$ ) or FAAH<sup>-/-</sup> mice (25–30 g, pure C57BL/6J background;  $n = 3$ ) and cultured as described previously (50). All animals received humane care, and all procedures were approved by the local committees for animal studies (Regierungspräsident Karlsruhe and Cologne).

**Experimental models of liver fibrosis.** Liver fibrosis was induced in male C57BL/6J wild-type mice by intraperitoneal injections of CCl<sub>4</sub> (0.5  $\mu$ l/g body wt; 1:1 dilution with sterile mineral oil) twice a week for 4 wk (48). Control mice were treated with mineral oil alone (0.5

$\mu$ l/g body wt; 1:1 dilution with sterile PBS). For analysis of in vivo-activated primary HSCs, we applied a model of cholestatic liver fibrosis (3). Briefly, BDL or sham operation was performed in male Sprague-Dawley rats ( $n = 3$  each; 350–400 g). After midline laparotomy, the common bile duct was ligated with 4–0 silk two times and transected between the two ligations. The sham operation was performed likewise, with the exception of ligating and transecting the bile duct.

**Isolation of dorsal root ganglia.** As a positive control for TH-expressing tissue, we used dorsal root ganglia (9). C57BL/6J wild-type mice (25–30 g) were killed by cervical dislocation. The spines of three mice were dissected and placed in a sterile culture dish. After the spine was opened, the dorsal root ganglia were dissected under a binocular microscope. The ganglia were carefully stripped of connective tissue with fine forceps and processed further mRNA isolation as described below.

**TH immunohistochemistry.** Human liver specimens were obtained according to the guidelines of the University of Bonn Ethics Committee from patients who had given their written informed consent. A paraffin-embedded liver biopsy specimen with normal liver histology or liver fibrosis due chronic hepatitis C virus infection (Desmet stage F1) was examined ( $n = 4$  each). Moreover, normal livers of vehicle-treated or fibrotic livers of CCl<sub>4</sub>-treated mice for 4 wk were examined ( $n = 4$ ). Immunohistochemistry using the TH antibody (Cayman Chemical, Ann Arbor, MI) in 1:200 dilution was performed on 4- $\mu$ m-thick paraffin-embedded sections by use of the peroxidase-conjugated avidin-biotin method following standard procedures (55).

**Measurement of endocannabinoid tissue levels.** The levels of NADA were measured in rat striatum ( $n = 4$ ), liver tissue from CCl<sub>4</sub>-treated mice for 21 days or controls ( $n = 8$  each), liver tissue from male Sprague-Dawley rats 21 days after BDL or sham operation ( $n = 8$  each), as well as in liver tissue from the above described human liver samples (normal or fibrotic livers, F1;  $n = 4$  each) by liquid chromatography/mass spectrometry. The measurement was performed as previously described (22) with a minor modification: to monitor NADA and the deuterated internal standard two additional precursor-to-product ion transitions were added to the mass spectrometry method, i.e.,  $m/z$  440.3  $\rightarrow$  137.0 for NADA and  $m/z$  448.3  $\rightarrow$  137.0 for NADA-d8. The levels of AEA were determined as previously described (48) in rat striatum ( $n = 4$ ) and in normal or fibrotic rat livers 21 days after BDL or sham operation ( $n = 8$  each).

**Treatment of cells and detection of cell death.** Cells were serum starved with DMEM containing 0.5% FCS for 12 h and treated either with NADA, AEA, or vehicle (ethanol; 0.1% final concentration), arachidonic acid, dopamine (all from Sigma-Aldrich, Deisenhofen, Germany), or actinomycin D (Sigma-Aldrich) plus murine TNF- $\alpha$  (R&D Systems, Minneapolis, MN). Where indicated, cells were pretreated with the pan-caspase inhibitor Val-Ala-Asp-fluoromethylketone (Z-VAD-FMK; R&D Systems); JNK inhibitor SP600125, FAAH inhibitor URB597, or CB1 antagonist AM251 (all Cayman Chemical, Ann Arbor, MI); CB2 antagonist SR144528 (Sanofi-Aventis, Montpellier, France); catechol-*O*-methyl-transferase (COMT) inhibitor OR-486 or receptor-interacting protein 1 (RIP1) inhibitor necrostatin-1 (both Tocris Bioscience, Bristol, UK); or TRPV1 antagonist capsazepine, TRPV1 agonist capsaicin, membrane cholesterol depletor methyl- $\beta$ -cyclodextrin, the antioxidants cell-permeable glutathione ethyl ester or Trolox, or the  $\gamma$ -glutamyl cysteine synthase inhibitor DL-buthionine-(S,R)-sulfoximine (BSO; all Sigma-Aldrich). Cell death in HSCs and hepatocytes was measured by LDH release into the culture medium according to the manufacturer's instructions (Roche Diagnostics, Mannheim, Germany) and by propidium iodide (PI; Sigma-Aldrich) fluorescence. Apoptosis and necrosis were visualized by fluorescent microscopy of PI and annexin V staining (Roche) according to the manufacturer's instructions.

**Detection of ROS.** Serum-starved HSCs ( $2 \times 10^4$  cells/well) plated in 24-well plates were loaded with the redox-sensitive dye 5-(and-6)-chloromethyl-2',7'-dichlorodihydrofluorescein diacetate (Molecular

Probes-Invitrogen, Darmstadt, Germany) for 30 min at 37°C, washed, and stimulated with NADA or AEA. ROS formation was measured for the indicated time in a multiwell fluorescence plate reader (Fluostar Optima; BMG, Offenburg, Germany) using excitation and emission filters of 485 and 535 nm, respectively (48, 50, 51).

**Western blot analysis.** Electrophoresis of protein extracts and subsequent blotting were performed as described previously (48, 50, 51). Blots were incubated with anti-TH, anti-FAAH (both Cayman Chemical); anti-caspase-3, anti-poly-(ADP-ribose) polymerase (anti-PARP), anti-phospho-ERK1/2, anti-AKT, anti-phospho-AKT (Thr308), anti-phospho-NF- $\kappa$ B p65 (Ser536), anti-phospho-JNK, or anti-RIP (all Cell Signaling Technologies, Beverly, MA, USA); or anti-COMT antibodies (Santa Cruz Biotechnology, Santa Cruz, CA) at a dilution of 1:1,000 or with anti- $\alpha$ -smooth muscle actin ( $\alpha$ -SMA; Sigma) at a dilution of 1:2,000 overnight at 4°C. After incubation with secondary horseradish-peroxidase conjugated antibody (Santa Cruz Biotechnology), the bands were visualized by the enhanced chemiluminescence light method (Amersham Biosciences) and exposed to X-omat film (Eastman Kodak, New Haven, CT) or a chemiluminescence imager (Image Station 2000R; Eastman Kodak). Blots were reprobbed with anti- $\beta$ -actin mouse antibody (MP Biomedicals, Santa Ana, CA) as an internal control. Where indicated, the intensities of the detected bands were evaluated densitometrically using ImageJ (NIH, Bethesda, MD).

**Quantitative RT-PCR analysis.** RNA was extracted by the TRIzol method (Invitrogen, Darmstadt, Germany). After DNase treatment, RNA was reverse transcribed into complementary DNA using random hexamer primers as described previously (50) and subsequently analyzed with the gene expression assay for TH (Applied Biosystems, Darmstadt, Germany; assay no. Mm00447557\_m1). The PCR reaction was performed with a universal PCR master mix (Applied Biosystems) through the amplification of 10 ng of complementary DNA for 40 cycles (95°C for 15 s and 60°C for 1 min) on an ABI-Prism 7900HT sequence detection system. Each sample was measured in duplicate, and quantification was performed by comparing the threshold cycle ( $C_t$ ) values of each sample to a standard curve. Gene expression was normalized to 18S and is expressed as fold induction compared with hepatocytes or whole liver, respectively.

**Wound healing assay.** HSCs were cultured to confluence (>90%) in sixwell plates. After starvation with DMEM containing 0.5% FCS for 12 h, a 2-mm-wide linear wound in the cell monolayer was created using a pipette tip (4). Cells were treated once daily with sublethal concentrations of NADA or vehicle only. Cells migrating into the wound were detected using a phase-contrast microscope at days 0, 4, and 6.

**Adenoviral infection.** Construction of adenoviruses expressing fatty acid amid hydrolase (AdFAAH) or a green fluorescent protein-expressing control virus (AdGFP) have been previously described (50). Rat HSCs were infected with AdFAAH or AdGFP at a multiplicity of infection of 50, achieving transduction rates of  $\geq 90\%$ . Cells underwent treatment with either NADA or AEA 24 h after initial infection.

**Measurement of adenosine triphosphate levels.** Human HSCs ( $4 \times 10^4$  cells/well) were exposed to 25 and 100  $\mu$ M NADA for 30 min or TNF- $\alpha$ /actinomycin D for 8 h. Cells were still alive and attached to the plate. Cellular ATP levels were quantified using a luciferin- and luciferase-based assay. Cells were rinsed with PBS and lysed with ATP-releasing buffer containing 100 mM potassium phosphate buffer at pH 7.8, 2 mM EDTA, 1 mM dithiothreitol, and 1% Triton X-100. ATP concentrations in lysates were quantified using an ATP determination kit (Invitrogen) according to the manufacturer's instructions and normalized to protein content.

**Statistical analysis.** All data represent the mean of three independent experiments  $\pm$  SE, if not otherwise stated. For the determination of statistical significance, unpaired Student's *t*-tests were performed using SigmaStat (SPSS, Chicago, IL). *P* values of <0.05 were considered to be statistically significant.

## RESULTS

*Mainly sympathetic neurons in the liver express the rate-limiting NADA-synthesizing enzyme TH.* We found that TH as the rate-limiting NADA-producing enzyme was expressed in healthy liver as well as in injured and fibrotic liver of wild-type mice that have been treated with intraperitoneal injections of CCl<sub>4</sub> for 4 wk (Fig. 1A). Interestingly, hepatocytes, but not activated HSCs, highly expressed TH (Fig. 1B). In a quantitative RT-PCR analysis, hepatocytes expressed significantly higher mRNA levels of TH than the nonparenchymal cell populations HSCs, Kupffer cells, or LSECs (Fig. 1C). However, TH mRNA levels of normal liver were  $\sim 1,800$  times lower compared with dorsal root ganglion tissue that contains sympathetic neurons (9; Fig. 1D). Accordingly, immunohistochemistry revealed sympathetic neurons in portal tracts as the main TH-expressing cell population in normal and fibrotic mouse or human liver (Fig. 1E). Thus predominantly sympathetic neurons in the liver hold the enzymatic machinery to produce NADA in normal and fibrotic livers. After identification of the potential NADA-synthesizing liver cell population, we further sought to evaluate the liver tissue levels of the endocannabinoids NADA and AEA. Since NADA has previously been discovered and detected in rat striatum (8, 24), we used this tissue to establish the method to measure NADA as well as AEA in normal and fibrotic liver tissue from mouse, rat, or humans. We found an approximate tissue level of NADA in rat striatum ( $n = 4$ ) of 1.0 nM and AEA of 30.1 nM (Fig. 1F, left). As previously described, NADA proved to be a very volatile molecule in peripheral tissues, including human plasma (1, 53). Thus we were not able to measure NADA levels in the livers of neither species. However, AEA was detectable in normal rat liver ( $n = 8$ ) at a level of 1.0 nM. In fibrotic livers (21 days after BDL), AEA was significantly upregulated to 2.9 nM, indicating the activation of the endocannabinoid system during liver injury and fibrogenesis (Fig. 1F, right).

*NADA efficiently mediates cell death in activated rat, mouse, and human HSCs.* After addition to the culture media, NADA rapidly and dose dependently induced cell death in rat HSCs (Fig. 2A). After 2 h of NADA treatment, 23, 34, 55, and 69% of rat HSCs underwent cell death at concentrations of 10, 25, 50, and 100  $\mu$ M, respectively. Cell death was induced significantly after 4 h at NADA concentrations starting at 10  $\mu$ M. Cell death reached plateau levels after 4 h at NADA concentrations of 50  $\mu$ M and higher achieving a maximum of 86%. Concentrations <5  $\mu$ M did not induce significant death in HSCs during exposure time of up to 24 h. Similar results were obtained in primary mouse HSCs (Fig. 2B) as well as in primary human HSCs (Fig. 2C), which were even more susceptible towards NADA-induced cell death. Since especially NADA appeared to have a very short half life, we tested whether NADA was also able to induce cell death in activated HSCs after a very short time of exposure. Indeed, after an exposure time of 30 s, NADA led to similar induction of cell death than after an exposure time of 2 h (Fig. 2D).

*NADA effectively induces cell death in in vivo-activated HSCs.* Since in vivo-activation of HSCs is considered to be the gold standard for the study of HSC biology (14) and to exclude the possibility that culture activation of HSCs artificially modulated their sensitivity to NADA-induced death, we performed

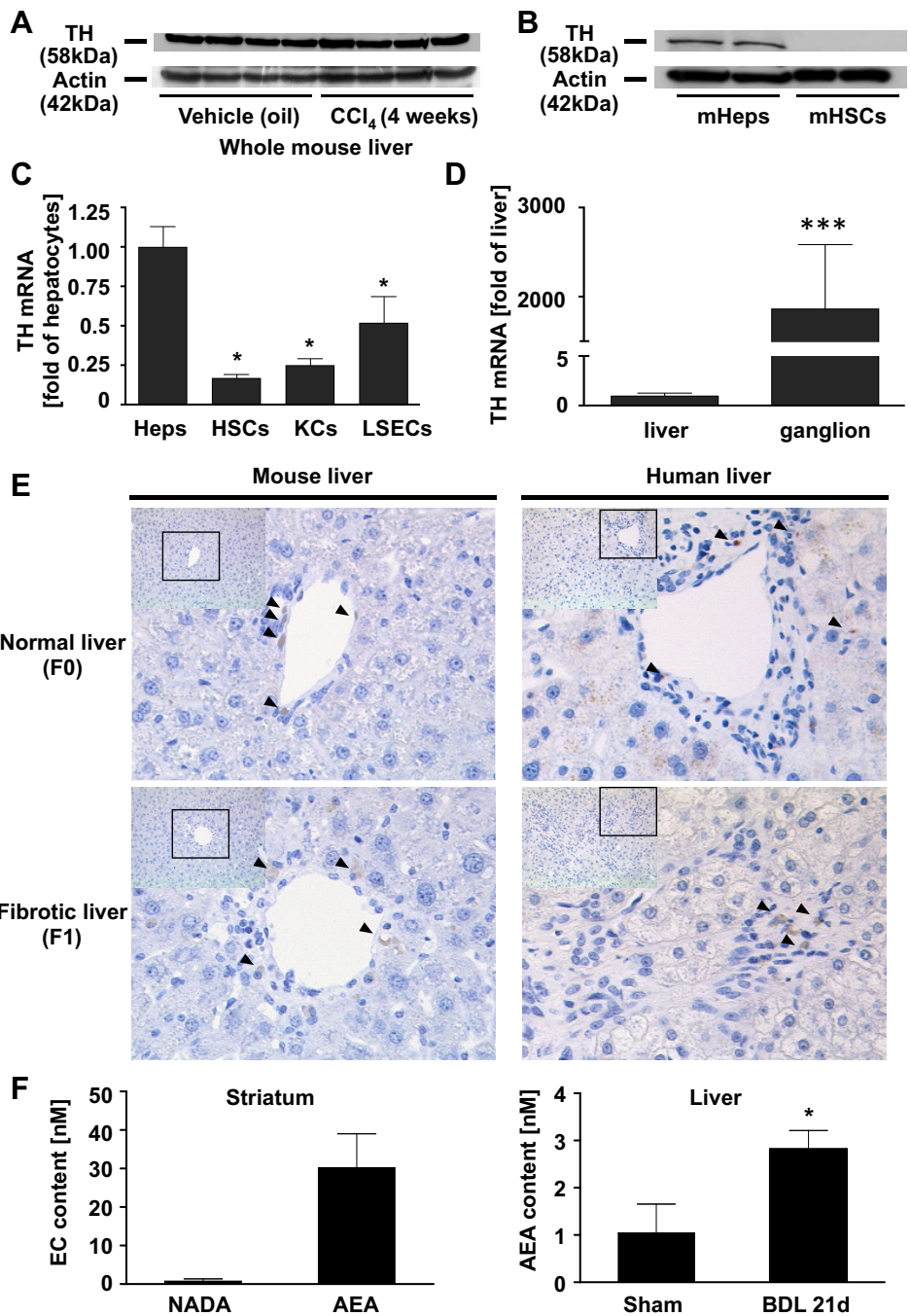


Fig. 1. Levels and expression patterns of the rate-limiting *N*-arachidonoyl dopamine (NADA)-synthesizing enzyme tyrosine hydroxylase (TH) and endocannabinoids in normal and fibrotic liver. **A**: male C57BL/6J mice ( $n = 4$ ) underwent peritoneal carbon tetrachloride (CCl<sub>4</sub>) administration for 4 wk twice a week for fibrosis induction. TH expression was compared with control mice ( $n = 4$ ) by Western blotting. **B**: expression of TH was compared in 2 independent isolations of primary mouse hepatocytes and activated primary mouse HSCs by Western blotting. **C**: TH mRNA levels were determined by quantitative RT-PCR in primary mouse hepatocytes (mHeps), hepatic stellate cells (mHSCs), Kupffer cells (KCs), and liver sinusoidal endothelial cells (LSECs;  $n = 3$  independent cell isolations; \* $P < 0.05$  vs. hepatocytes). **D**: TH mRNA levels were determined by quantitative RT-PCR in whole normal mouse liver as well as in dorsal root ganglia ( $n = 3$ ; \*\*\* $P < 0.0001$  vs. whole mouse liver). **E**: immunohistochemistry for TH was performed in normal (F0) and fibrotic (F1) mouse or human liver. Arrows depict TH expression predominantly in sympathetic neurons. Representative fields were selected from slides with  $\times 100$  original magnification shown at *top left*. Final magnification =  $\times 400$ . **F**: endocannabinoids [EC; NADA and anandamide (AEA)] were measured in rat striatum (*left*;  $n = 4$ ), sham, or fibrotic liver [21 days after bile duct ligation (BDL); *right*;  $n = 8$  each] as described (\* $P < 0.05$  vs. sham). At least 3 independent experiments are shown.

BDL in rats for in vivo activation of HSCs. Twenty-one days after BDL, livers showed an increased expression of  $\alpha$ -SMA (Fig. 2E, *left*) as a sign of increased activation of HSCs, compared with livers of sham-operated rats. HSCs isolated from fibrotic livers of BDL-treated rats showed an activated phenotype (Fig. 2E, *middle*) and considerably higher expression of  $\alpha$ -SMA (Fig. 2E, *right*) in contrast to HSCs isolated from sham-operated rat livers. In vivo-activated HSCs were treated with NADA 24 h after isolation and were extremely sensitive to NADA-mediated cell death: HSCs already started to undergo cell death at concentrations  $< 5 \mu\text{M}$  2 h after treatment (Fig. 2F) and were efficiently killed after 4 h

even at low concentrations of NADA (almost 60% cell death at  $10 \mu\text{M}$ ).

*NADA induces necrosis, but not apoptosis, in activated HSCs.* To determine whether cell death induced by NADA was apoptotic or necrotic, we treated rat HSCs with either NADA, AEA, or actinomycin D and TNF- $\alpha$ . Similar to AEA and in contrast to the apoptotic control actinomycin D/TNF- $\alpha$ , NADA-treated HSCs displayed no annexin V staining but showed strong nuclear PI staining. Therefore, NADA-induced death appears to be necrotic (Fig. 3A). HSCs treated with NADA showed cleavage of caspase 3 as displayed by Western blot in Fig. 3B. However, caspase inhibition with the pan-caspase inhibitor

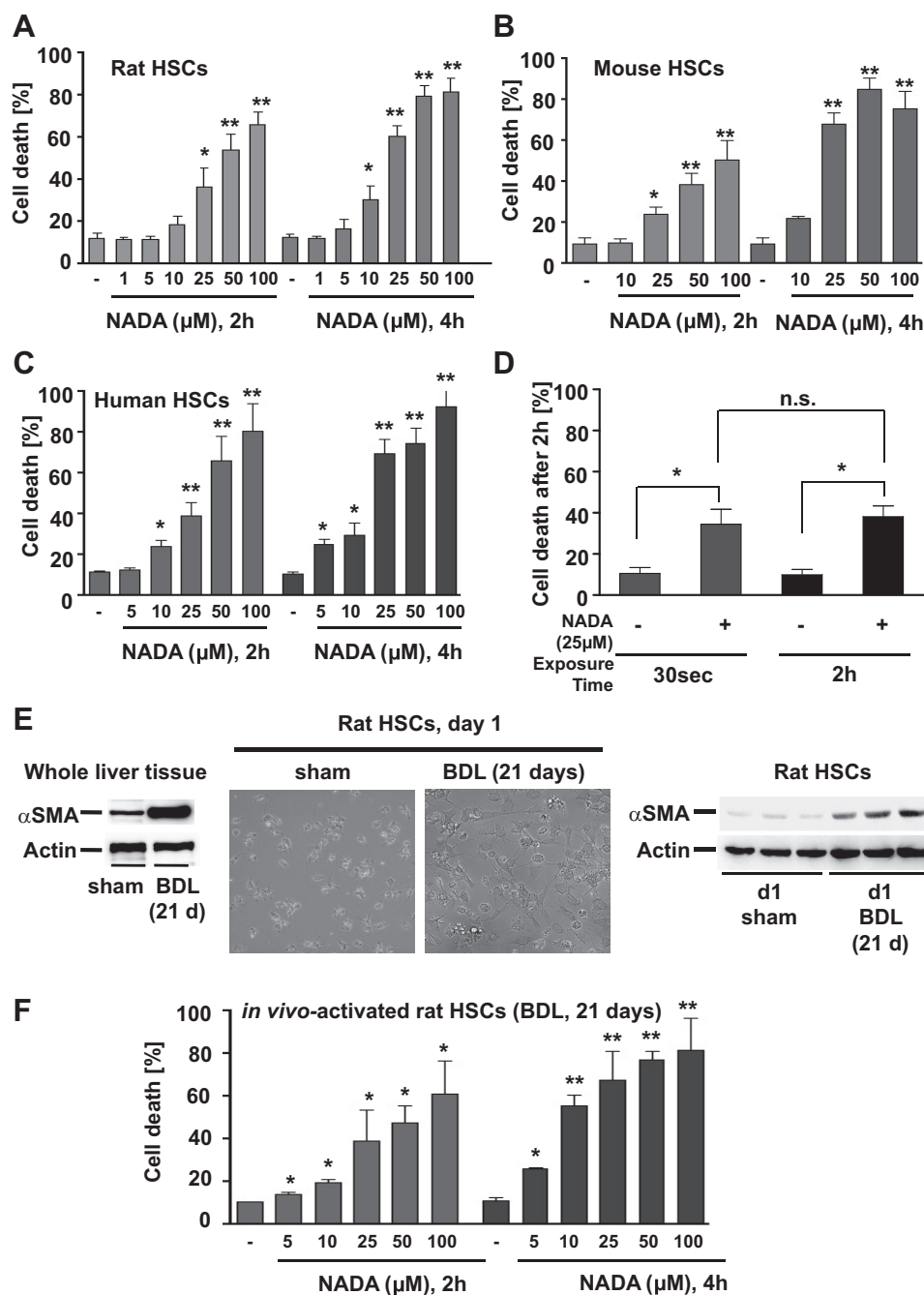


Fig. 2. NADA rapidly and dose dependently induces cell death in culture-activated primary HSCs of rats, mice, or humans and in vivo-activated primary rat HSCs. *A*: rat HSCs were serum-starved for 12 h and treated with the indicated concentrations of NADA or vehicle up to 4 h. Media were collected after 2 or 4 h of treatment, and cell death was determined by measuring the release of LDH into the media. Cell death is displayed as percentage of the maximum LDH release achieved by complete cell lysis with Triton-X 100 (\* $P < 0.05$ , \*\* $P < 0.001$  vs. vehicle treatment). *B* and *C*: mouse or human HSCs were equally treated as described in *A*. Cell death was analyzed by LDH release assay in the culture media (\* $P < 0.05$ , \*\* $P < 0.001$  vs. vehicle treatment). *D*: human HSCs were exposed for 30 s to NADA (25  $\mu$ M) before the culture media were changed and the cells were washed 3 times with fresh media or were treated with the same concentration of NADA for 2 h without the media being changed. After 2 h, cell death was analyzed by LDH assay (\* $P < 0.05$  vs. vehicle treatment). *E*: HSCs were isolated from rat livers 21 days (d) after sham operation or BDL (phase contrast; *middle*; 24 h after isolation). Intrahepatic HSC activation in BDL-treated livers is indicated by Western blot for  $\alpha$ -smooth muscle actin ( $\alpha$ -SMA) vs. sham in whole liver (*left*) and after isolation of HSCs from BDL-treated livers vs. HSCs from sham-operated rats (*right*;  $n = 3$  each). *F*: 24 h after isolation (*day 1*) in vivo-activated rat HSCs were treated with vehicle or increasing concentrations of NADA for 2 or 4 h. Cell death was analyzed by LDH assay (\* $P < 0.05$ , \*\* $P < 0.001$  vs. vehicle treatment). At least 3 independent experiments are shown.

Z-VAD-FMK did not inhibit NADA-induced cell death in HSCs in contrast to TNF- $\alpha$ /actinomycin D, indicating a caspase-independent form of cell death (Fig. 3C). Moreover, NADA failed to induce PARP cleavage in HSCs as another hallmark of apoptotic cell death (data not shown), indicating that NADA-mediated cell death was indeed necrotic. To further examine, whether NADA-induced cell death involved features of programmed necrosis/necroptosis (56), we analyzed the expression of RIP1. RIP1 is essentially required for initiation of programmed necrosis and appeared to be slightly upregulated 60 min after NADA treatment (Fig. 3D, *left*). However, treatment with the RIP1-inhibitor necrostatin-1 did not inhibit NADA-induced cell death (Fig. 3D, *right*). There-

fore, NADA did not induce necroptosis. Furthermore, NADA-treatment led to early depletion of ATP in contrast to the proapoptotic treatment with actinomycin D/TNF- $\alpha$ , underlining the plain necrotic nature of NADA-caused cell death in HSCs (Fig. 3E).

We further sought to analyze the signaling pathways involved in NADA-induced cell death and whether signaling pathways promoting stellate cell survival were possibly inhibited by NADA. Since we and others (32, 51) previously showed that AEA treatment in HSCs led to an activation of the JNK pathway, which may contribute to cell death, we performed Western blotting for phospho-JNK. NADA as well as PDGF-BB as positive control led to JNK phosphorylation (Fig.

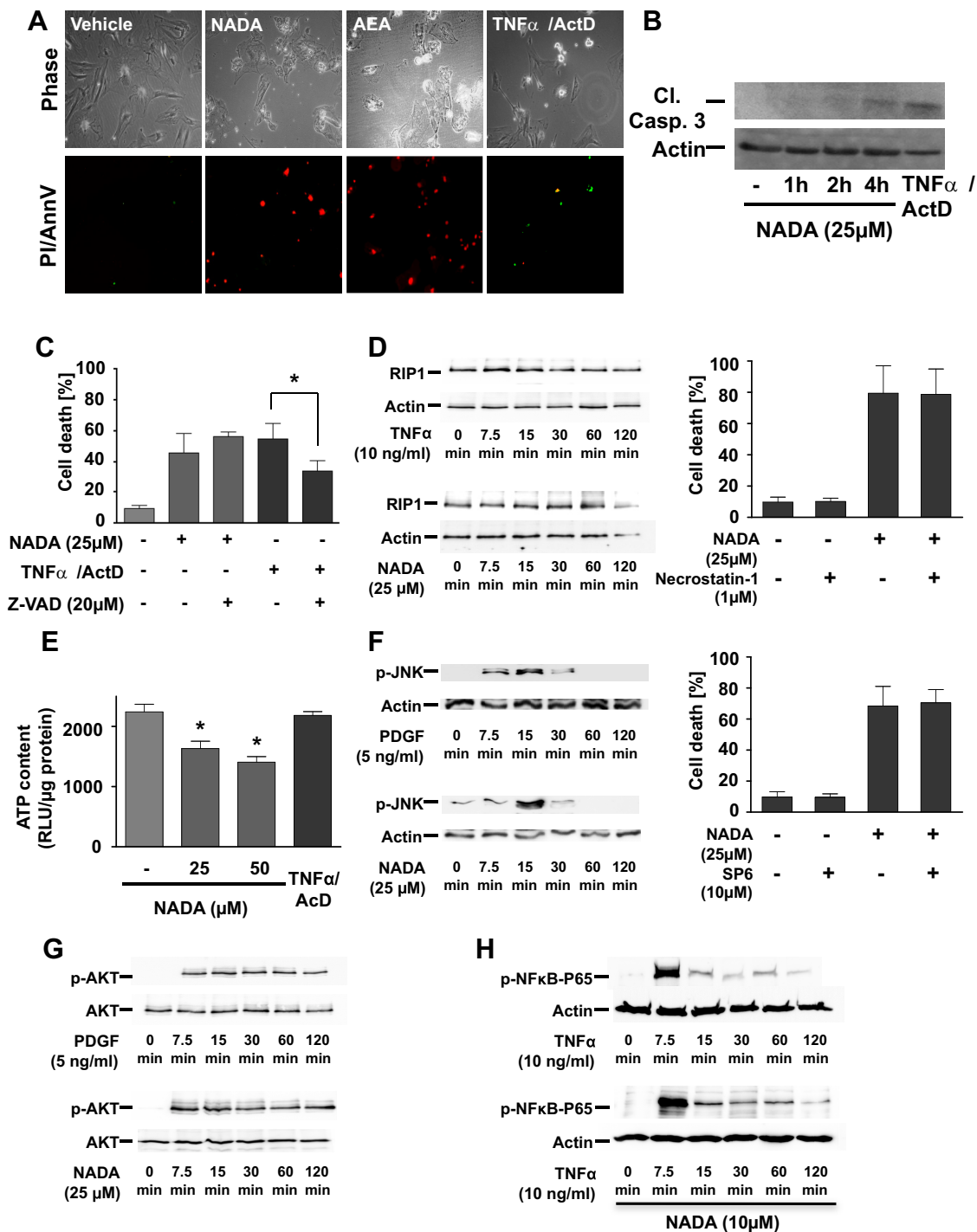


Fig. 3. NADA induces pure necrotic cell death due to depletion of cellular ATP stores. *A*: rat HSCs were serum starved for 12 h and treated with either 25  $\mu$ M NADA or AEA for 4 h or with actinomycin D (ActD; 0.2  $\mu$ g/ml) plus TNF- $\alpha$  (10 ng/ml) for 16 h as a positive control for apoptotic cell death. Apoptotic cell death was indicated by green fluorescence of annexin V (AnnV), and necrotic cell death is shown by red staining of the nuclei by propidium iodide (PI). *B*: primary rat HSCs were treated with NADA (25  $\mu$ M) for the indicated time or with ActD plus recombinant murine (rm)TNF- $\alpha$  (ActD/TNF- $\alpha$ ) for 12 h as positive control. Western blot was performed with antibodies directed against caspase 3 and  $\beta$ -actin. *C*: mouse HSCs were pretreated with the pan-caspase inhibitor Val-Ala-Asp-fluoromethylketone (Z-VAD-FMK; 20  $\mu$ M) for 30 min followed either by incubation with ActD/TNF- $\alpha$  for 12 h or treatment with AEA (25  $\mu$ M) for 4 h. Cell death was measured by LDH assay (\* $P$  < 0.05 vs. ActD/rmTNF- $\alpha$  alone). *D*: mouse HSCs were treated with TNF- $\alpha$  (10 ng/ml) as a positive control or NADA (25  $\mu$ M) for the indicated time. *Left*: Western blotting was performed with antibodies directed against receptor-interacting protein (RIP) and actin. *Right*: cells were pretreated with vehicle or the RIP1-inhibitor necrostatin-1 (1  $\mu$ M) for 30 min before NADA exposure (25  $\mu$ M) for 4 h. *E*: ATP content of human HSCs was analyzed by the luciferin method in triplicates as described (\* $P$  < 0.05 vs. vehicle treatment). *F*: mouse HSCs were treated with PDGF-BB (5 ng/ml) as a positive control or NADA (25  $\mu$ M) for the indicated time. *Left*: Western blotting was performed with antibodies directed against phospho-JNK and actin. *Right*: cells were pretreated with vehicle or the JNK-inhibitor SP600125 (SP6; 10  $\mu$ M) for 30 min before NADA-exposure (25  $\mu$ M) for 4 h. *G*: mouse HSCs were treated with PDGF-BB (5 ng/ml) as a positive control or NADA (25  $\mu$ M) for the indicated time. Western blotting was performed with antibodies directed against phospho-AKT and AKT. *H*: mouse HSCs were treated with TNF- $\alpha$  (10 ng/ml) as a positive control for the indicated time. To evaluate a putative inhibition of NF- $\kappa$ B activation by NADA, we pretreated the cells with NADA (25  $\mu$ M) for 30 min before TNF- $\alpha$ . Western blotting was performed with antibodies directed against phospho-NF- $\kappa$ B p65 and actin. At least 3 independent experiments are shown.

3F, left). However, pharmacological JNK inhibition through the small molecule inhibitor SP600125 did not reduce NADA-mediated cell death (Fig. 3F, right). Thus we could rule out a causative role of the JNK pathway in NADA-induced HSC death. Interestingly, NADA activated the AKT pathway, which is known to promote HSC survival (41), in a similar way as PDGF-BB (Fig. 3G). However, the apparent activation of this survival pathway was not sufficient to inhibit NADA-induced cell death. Moreover, activation of the NF- $\kappa$ B pathway has also been linked to HSC survival (41). We (51) have previously shown, that the endocannabinoid AEA was an inhibitor of TNF- $\alpha$ -induced NF- $\kappa$ B activation. NADA alone did not induce phosphorylation of the NF- $\kappa$ B subunit p65 (data not shown). To check for inhibition of NF- $\kappa$ B by NADA, we pretreated HSCs with NADA before TNF- $\alpha$  exposure. In contrast to AEA (51), NADA did not inhibit NF- $\kappa$ B p65 phosphorylation by TNF- $\alpha$  (Fig. 3). Conversely, NF- $\kappa$ B activation by TNF- $\alpha$  administration before NADA treatment did not inhibit NADA-induced cell death (data not shown). Thus the NF- $\kappa$ B pathway

was neither involved in NADA-induced cell death nor in survival signaling.

*Sublethal doses of NADA reduce activation, proliferation, and migration in HSCs.* Since we found that AEA was able to inhibit HSC proliferation in activated primary HSCs in sublethal doses (51), we tested the effects of NADA (1  $\mu$ M) on proliferation and migration of fully activated primary rat HSCs in a wound healing assay. Cells treated with vehicle only were able to proliferate and migrate into the wound to nearly close it after 6 days. NADA treatment, however, almost completely inhibited HSC proliferation and migration (Fig. 4A). To elucidate the mechanism behind the inhibition of HSC proliferation and migration, we examined the effect of NADA on proliferative signaling. Incubation of HSCs with 10% FBS in the culture media led to marked ERK1/2 phosphorylation, which could be inhibited by exposure of the cells to NADA (0.1  $\mu$ M; Fig. 4B). We further sought to investigate whether exposure to sublethal concentrations of NADA prevented activation of primary HSCs. Interestingly, we were able to detect

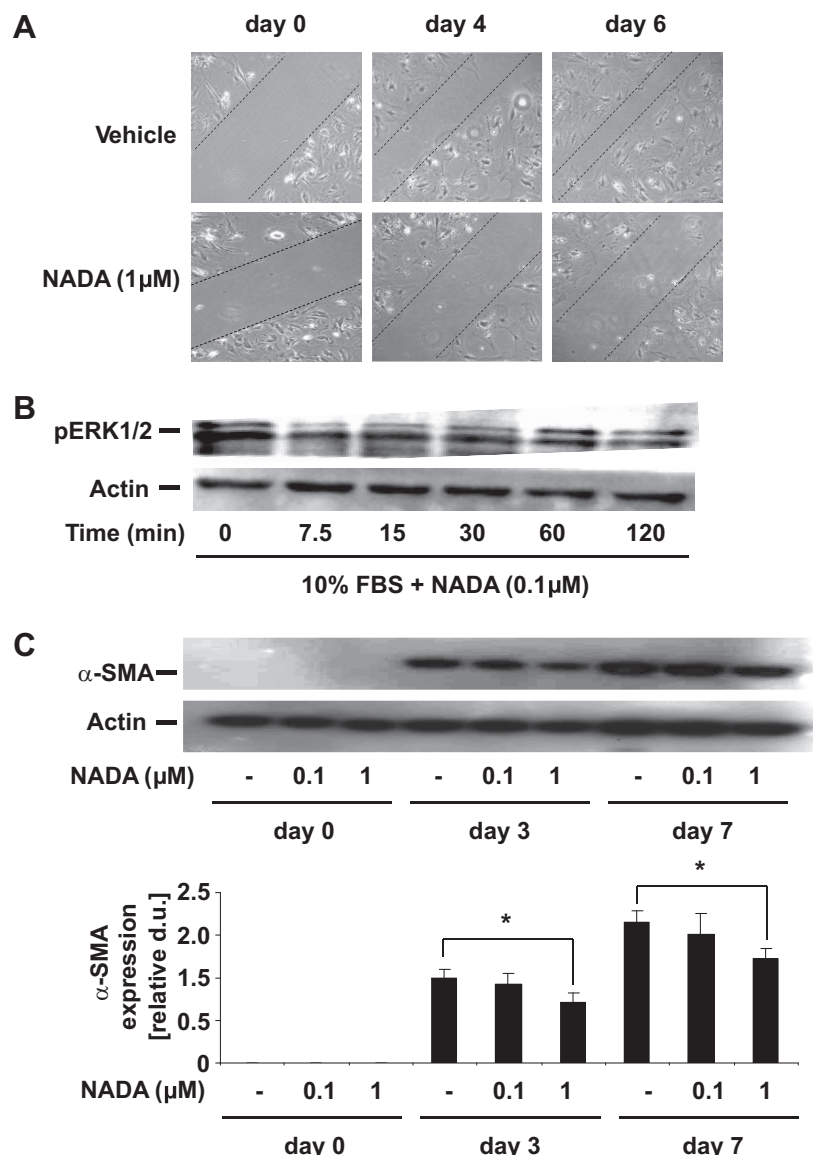


Fig. 4. Sublethal doses of NADA reduce proliferation, migration, and activation of HSCs. *A*: wound healing assay was performed with a pipette tip through the cell monolayer of activated primary mouse HSCs. Phase contrast images were taken on *days 0, 4, and 6*. At least 3 independent experiments performed in duplicates are shown. *B*: activated primary mouse HSCs were cultured with DMEM culture media containing 10% FBS and were treated with NADA (100 nM) for the indicated times. Western blots for phospho-ERK1/2 and  $\beta$ -actin as loading control were performed. Blot represents 3 independent experiments. *C*: freshly isolated mouse HSCs were treated with the indicated concentrations of NADA or vehicle (–) daily for the indicated time. Cell culture media were renewed each day before the addition of NADA into the media. Western blots of  $\alpha$ -SMA monitoring the activation status of HSCs and  $\beta$ -actin as loading control are representative for three independent experiments. *Bottom*: densitometric quantifications are shown in means of relative densitometric units  $\pm$  SE (d.u.) compared with  $\alpha$ -SMA expression after vehicle treatment on *day 3* set to *day 1* (\* $P$  < 0.05 vs. vehicle;  $n$  = 3).

significantly lower expression of  $\alpha$ -SMA as a marker of HSC activation after daily treatment of freshly isolated primary mouse HSCs with NADA (1  $\mu$ M) in a time course of 7 days (Fig. 4C, *top* and *bottom*). At a dose of 0.1  $\mu$ M daily, this effect was still detectable, yet not statistically significant (Fig. 4C, *top* and *bottom*).

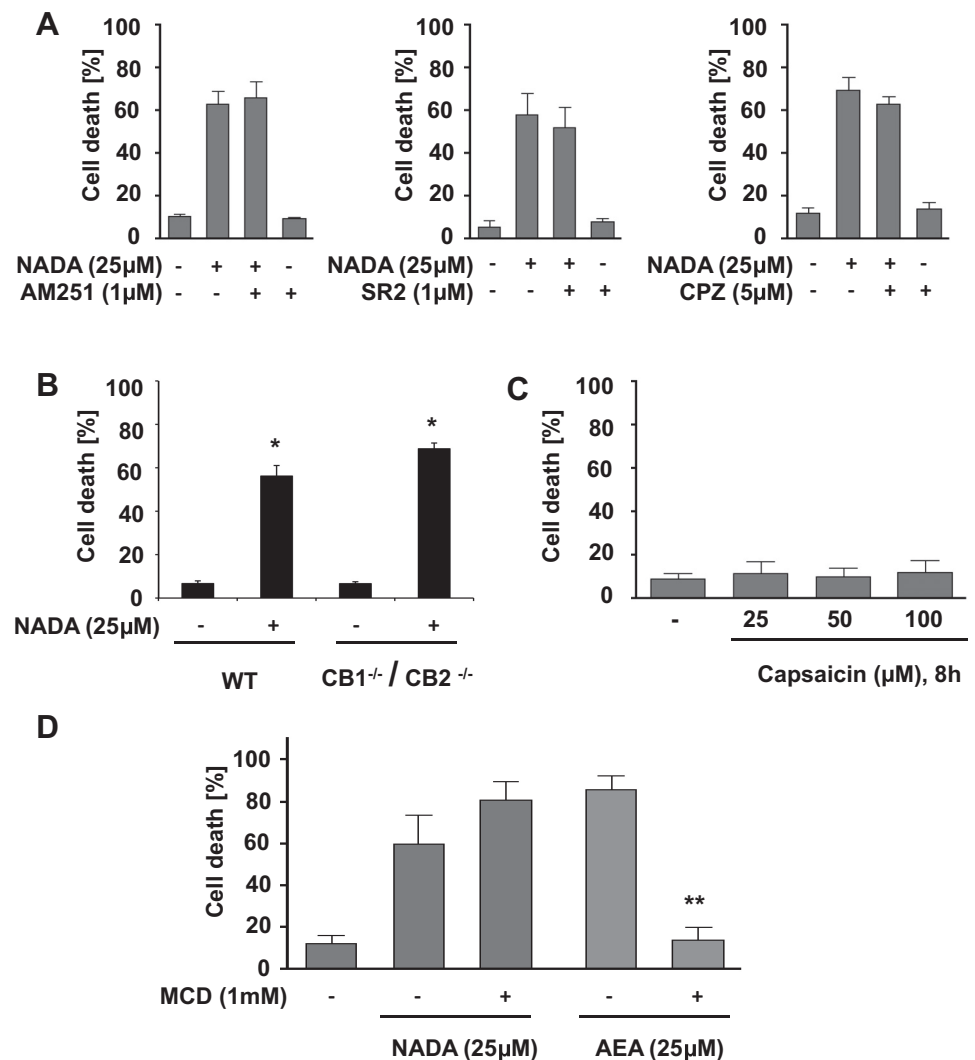
**NADA-induced death in HSCs occurs independently of the cannabinoid receptors CB1, CB2, or TRPV1.** NADA was shown to be a full agonist at CB1 receptors and TRPV1 receptors and to a lesser extent at CB2 receptors (6, 24). Since we have (51) previously shown that these receptors are expressed in HSCs, we investigated whether HSC death is mediated by these receptors in response to NADA using both pharmacologic and genetic approaches. NADA-induced cell death was neither blocked by AM251, a specific antagonist of CB1, nor by SR144528 (SR2), a specific antagonist of CB2, nor by capsazepine, a specific antagonist of TRPV1 (Fig. 5A), indicating that NADA induces cell death independently of these receptors. None of the inhibitors alone did induce cell death in HSCs (Fig. 5A). We further confirmed these findings in HSCs isolated from CB1/CB2<sup>-/-</sup> double knockout mice compared with HSCs from wild-type mice (Fig. 5B). Since several previous studies (13, 45) have shown that NADA

induced cell death in certain cell types via TRPV1 activation, we checked whether the specific TRPV1 agonist capsaicin induced cell death in primary activated mouse HSCs. In contrast to NADA, capsaicin did not induce cell death in doses up to 100  $\mu$ M in HSCs (Fig. 5C). This underlines the clear independence of NADA-mediated cell death from TRPV1 signaling.

**NADA-induced cell death does not depend on membrane cholesterol.** Various studies in several different cell types have shown that AEA induces cell death independently of CB1, CB2, or TRPV1 through interaction with membrane cholesterol, possibly via cholesterol-rich lipid rafts (15, 16). Accordingly, membrane cholesterol depletion by methyl- $\beta$ -cyclodextrin preincubation completely inhibited necrosis induced by 25  $\mu$ M AEA but not by 25  $\mu$ M NADA (Fig. 5D), indicating that NADA does not require interaction with membrane cholesterol for cellular uptake and subsequent induction of cell death in HSCs.

**NADA-induced necrosis depends on intracellular ROS formation.** NADA caused a marked and rapid increase in ROS formation (Fig. 6A) that occurred predominantly cytoplasmatically as well as intranuclearly (Fig. 6B). ROS generation induced by NADA was dose dependent, and the extent was

Fig. 5. NADA-induced killing of HSCs is not mediated by cannabinoid receptor type 1 and 2 (CB1 and CB2) and transient receptor potential cation channel subfamily V, member 1 (TRPV1) or membrane cholesterol. **A:** HSCs were incubated with the specific receptor antagonists AM251 (1  $\mu$ M; *left*), SR144528 (SR2; 1  $\mu$ M; *middle*) or capsazepine (CPZ; 5  $\mu$ M; *right*) for CB1, CB2, or TRPV1, respectively, 30 min before addition of NADA (25  $\mu$ M for 4 h). Cell death was analyzed by LDH assay. **B:** primary HSCs from wild-type (WT) or CB1<sup>-/-</sup>CB2<sup>-/-</sup> double knockout mice were treated with NADA (25  $\mu$ M) or vehicle for 4 h. Cell death was analyzed by LDH assay (\**P* < 0.05 vs. vehicle). **C:** primary mouse HSCs were treated with the indicated concentrations of the TRPV1 agonist capsaicin for 8 h. Cell death was analyzed by LDH assay. **D:** HSCs were incubated with the membrane cholesterol depletor methyl- $\beta$ -cyclodextrin (MCD; 1 mM) for 1 h and then stimulated with 25  $\mu$ M NADA or AEA. Cell death was analyzed by LDH assay (\*\**P* < 0.001 vs. AEA alone). At least 3 independent experiments are shown.



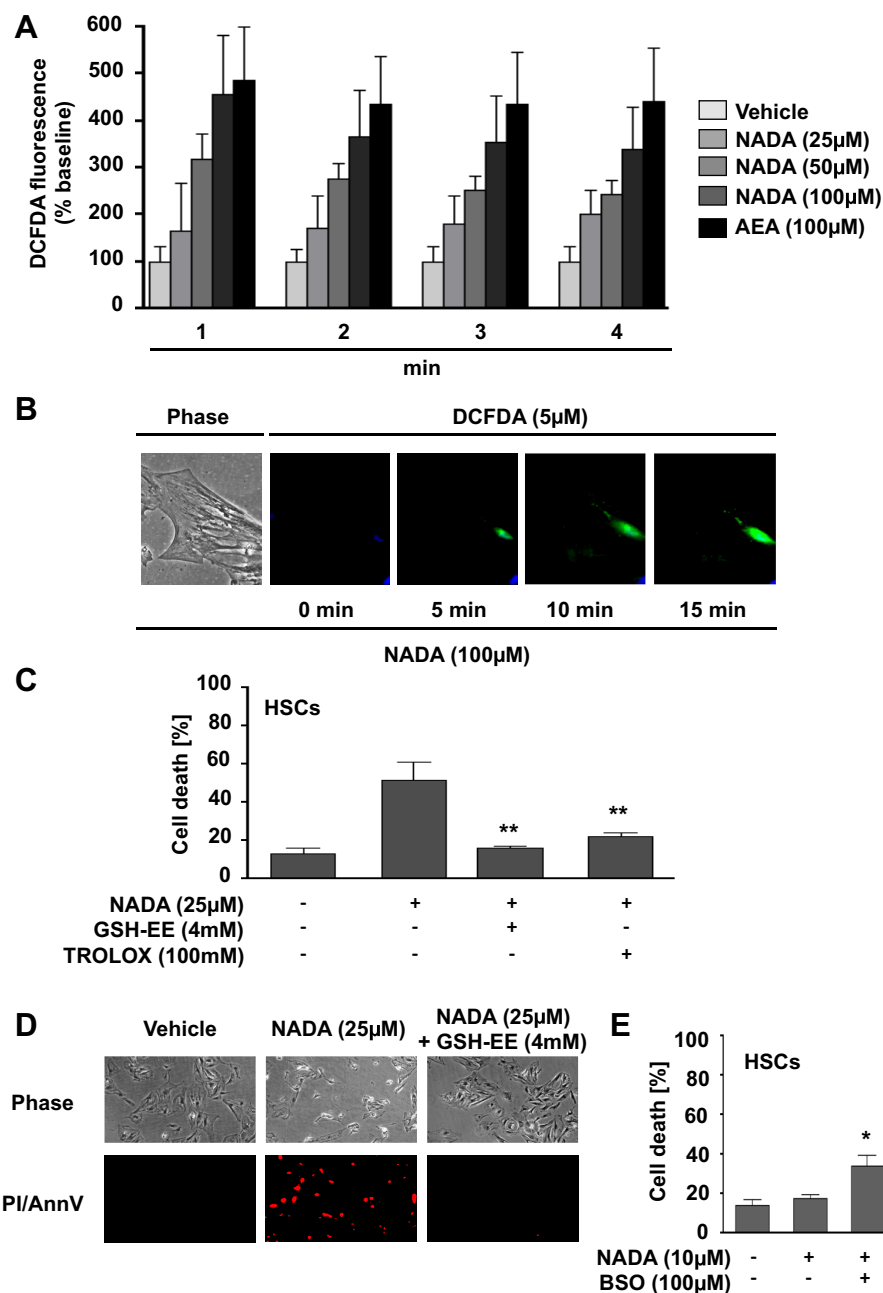


Fig. 6. Intracellular reactive oxygen species contribute to NADA-induced cell death. *A* and *B*: activated rat HSCs were loaded with 5-(and-6)-chloromethyl-2',7'-dichlorodihydrofluorescein diacetate (CM-H<sub>2</sub>DCFDA; 5 μM) for 30 min and treated with 25, 50, and 100 μM NADA, 100 μM AEA, or vehicle. Reactive oxygen species formation was measured in a multiwell plate-reader in quadruplicates (*A*) or the green fluorescence of CM-H<sub>2</sub>DCFDA was visualized in one single cell (*B*) for the indicated time. *C*: activated rat HSCs were preincubated with 4 mM glutathione ethyl ester (GSH-EE) or 100 mM Trolox and treatment with NADA (25 μM for 4 h). Cell death was analyzed by LDH assay (\*\**P* < 0.001 vs. NADA alone). *D*: after 1 h of pretreatment with GSH-EE (4 mM) or Trolox (100 mM), cells were exposed to NADA (25 μM for 4 h). Necrotic cell death is shown by the red staining of the nuclei by PI. *E*: activated HSCs were pretreated with DL-buthionine-(S,R)-sulfoximine (BSO; 100 μM) or vehicle 30 min before exposure to NADA (10 μM) for 2 h. Cell death was determined by LDH release assay (\**P* < 0.05 vs. NADA alone). At least 3 independent experiments are shown.

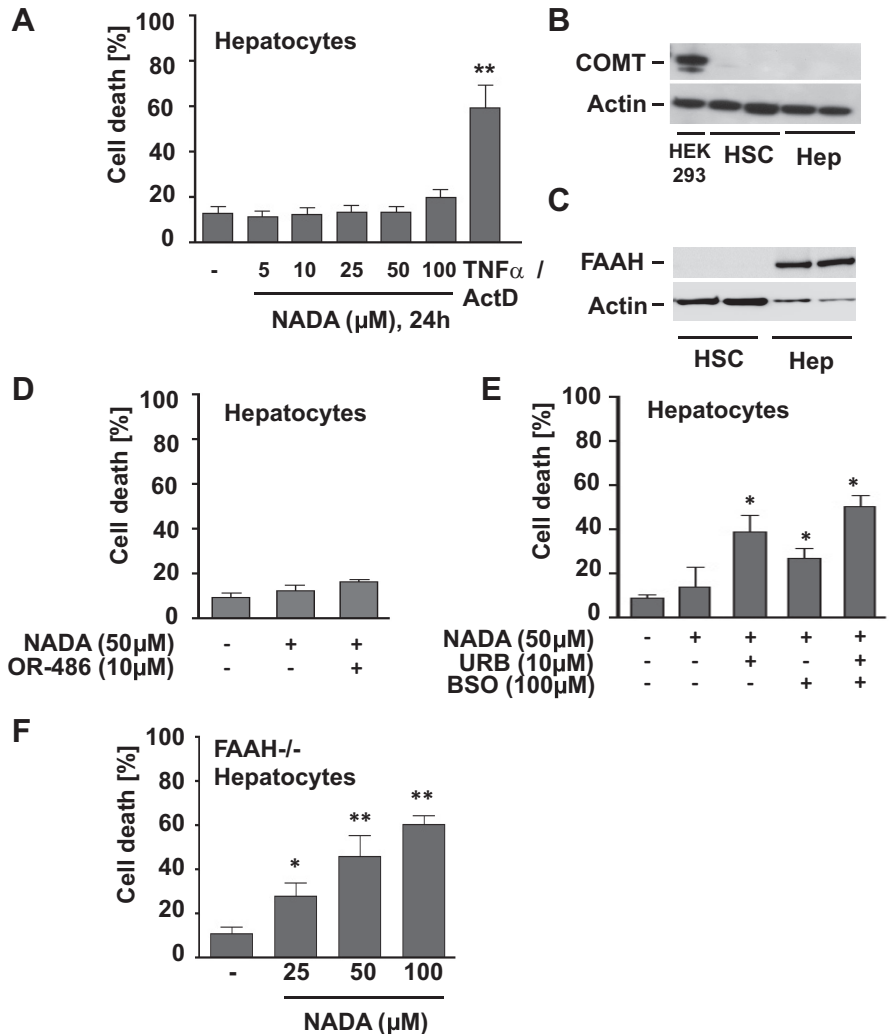
similar to that of AEA at same concentrations (Fig. 6A). Pretreatment with the antioxidants glutathione ethyl ester or Trolox significantly reduced NADA-mediated cell death (Fig. 6, *C* and *D*; *P* < 0.001 vs. NADA alone), indicating that ROS substantially contribute to NADA-induced cell death. To provide further evidence for ROS as a key mediator of cytotoxic NADA signaling, we tested the effects of GSH depletion on NADA-induced cell death in HSCs. We found a significant, nearly 50% increase in cell death after 2 h of NADA treatment (10 μM) in HSCs that had been depleted of GSH by pretreatment with the γ-glutamyl cysteine synthase inhibitor BSO (Fig. 6E; *P* < 0.05 vs. NADA alone), supporting our hypothesis that ROS mediate cytotoxic NADA signals.

*NADA does not induce cell death in primary hepatocytes.* To underline the antifibrotic potential of NADA by effective

induction of cell death in HSCs and to exclude possible adverse effects of NADA on parenchymal cells of the liver, we exposed primary rat hepatocytes to increasing concentrations of NADA for up to 24 h. In contrast to HSCs, primary rat hepatocytes were resistant against cell death up to 100 μM NADA for 24 h (Fig. 7A). We obtained similar results with primary mouse hepatocytes (data not shown). Thus the exorbitant differences in cell death susceptibility of HSCs and hepatocytes imply that NADA selectively induces cell death in the main fibrogenic cells of the liver but not in hepatocytes.

*FAAH determines resistance to NADA-mediated death in hepatocytes.* Next, we examined the mechanisms behind this discrepancy of cell death susceptibility towards NADA of HSCs and hepatocytes. First we checked whether primary mouse HSCs or hepatocytes express COMT, which has previ-

Fig. 7. Fatty acid amide hydrolase (FAAH) and anti-oxidant expression are involved in the resistance to NADA-induced cell death. *A*: serum-starved primary rat hepatocytes were treated with vehicle (–) or NADA (10–100  $\mu$ M) for 24 h. Cell death was determined by LDH release (\*\* $P$  < 0.001 vs. vehicle). *B*: catechol-*O*-methyl-transferase (COMT) protein expression was analyzed in HEK293 cells (positive control), primary mouse HSCs and hepatocytes by Western blotting. *C*: FAAH protein expression was analyzed in primary mouse HSCs and hepatocytes by Western blotting. *D*: hepatocytes were either pretreated with the selective COMT inhibitor OR-486 (10  $\mu$ M) or vehicle for 1 h, followed by NADA (50  $\mu$ M) for 24 h. Cell death was determined by LDH release (\* $P$  < 0.05 vs. vehicle). *E*: primary mouse hepatocytes were either pretreated with vehicle or the selective FAAH inhibitor URB597 (10  $\mu$ M), BSO (100  $\mu$ M), or both substances for 1 h followed by NADA (25  $\mu$ M) for 24 h. Cell death was determined by LDH release (\* $P$  < 0.05 vs. vehicle). *F*: cell death in FAAH<sup>-/-</sup> hepatocytes after treatment with indicated NADA concentrations was determined by LDH release (\* $P$  < 0.05, \*\* $P$  < 0.001 vs. vehicle). At least 3 independent experiments are shown.



ously been described as a NADA-degrading enzyme (24). Neither HSCs nor hepatocytes showed a detectable expression of COMT (Fig. 7*B*). Conversely, primary mouse hepatocytes expressed large amounts of FAAH in contrast to HSCs (Fig. 7*C*), which has been also attributed to NADA degradation (24). When we applied NADA to hepatocytes that had been pretreated with the selective COMT inhibitor OR-486, we were not able to detect a significant induction of cell death (Fig. 7*D*). Thus we could rule out any contribution of this NADA degradation enzyme to the different susceptibility toward NADA-induced cell death in HSCs and hepatocytes. To investigate whether the differential expression of FAAH may contribute to the resistance of hepatocytes to NADA-induced cell death, we blocked FAAH activity by preincubation with URB597, a highly selective FAAH inhibitor (Fig. 7*E*). Interestingly, URB597 increased NADA-induced cell death in hepatocytes up to 43% at a concentration of 25  $\mu$ M. Incubation with URB597 alone did not induce any cell death (data not shown). This significant contribution of FAAH to the remarkable resistance of hepatocytes against NADA-induced cell death could be confirmed in FAAH<sup>-/-</sup> hepatocytes. Hepatocytes lacking FAAH were highly susceptible towards NADA with 28, 46, and 61% of dead cells after 10, 25, and 50  $\mu$ M NADA,

respectively (Fig. 7*F*). To further investigate the role of FAAH, rat HSCs were infected with an adenovirus expressing rat FAAH, which allowed us to overexpress this enzyme in HSCs. Infection resulted in a strong expression of FAAH (Fig. 8*A*). AdFAAH treatment of HSCs decreased NADA-induced cell death (25  $\mu$ M) from 55 to 23%, similarly to AEA-induced cell death (Fig. 7*C*). In contrast, HSCs infected with the control virus expressing only GFP showed no difference in NADA-induced cell death (Fig. 8, *B* and *C*). To exclude that NADA-induced cell death in primary HSCs was mediated by the putative metabolites of NADA, dopamine or arachidonic acid, and to finally prove that FAAH-mediated degradation of NADA into these metabolites terminates NADA toxicity, we incubated primary mouse HSCs with 25  $\mu$ M of each substance for 4 h (Fig. 8*D*). In contrast to NADA, neither arachidonic acid nor dopamine induced significant cell death. To further rule out that the induction of cell death in HSCs by NADA was an unspecific effect simply due to its nature as a reactive lipid mediator, we compared the substance to its precursor/metabolite arachidonic acid and to prostaglandin D<sub>2</sub> (PGD<sub>2</sub>), another alternative lipid molecule that is involved in a COX-2-dependent endocannabinoid metabolism pathway (29). Interestingly, even in high concentrations up

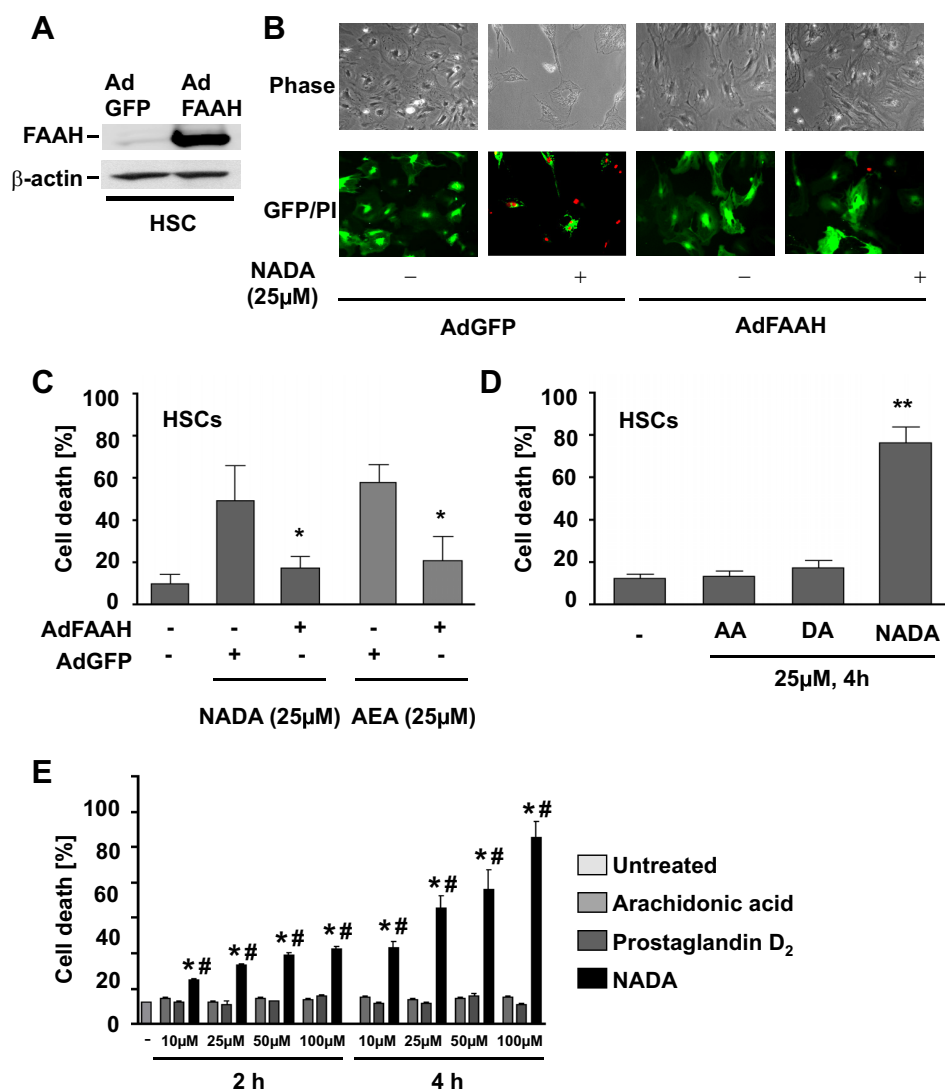


Fig. 8. FAAH overexpression rescues HSCs from NADA-induced cell death. *A*: expression of FAAH protein in rat HSCs infected with adenoviruses (Ad)FAAH or green fluorescent protein-expressing control virus (AdGFP) was determined by Western blotting. *B* and *C*: HSCs were infected with AdFAAH or AdGFP for 12 h and treated 24 h later with 25  $\mu$ M NADA or AEA for 4 h. Cell death was visualized by PI staining of the nuclei (*B*). Cell death in AdGFP-infected or AdFAAH-infected primary mouse HSCs after treatment with indicated NADA concentrations was determined by LDH release (\* $P$  < 0.05 vs. AdGFP; *C*). *D*: cells were treated with 25  $\mu$ M of arachidonic acid (AA), dopamine (DA), or NADA for 4 h. Cell death was assessed by LDH assay (\*\* $P$  < 0.001 vs. vehicle treatment). *E*: rat HSCs were serum-starved for 12 h and treated with the indicated concentrations of vehicle, NADA, arachidonic acid or PGD<sub>2</sub> up to 4 h. Media were collected, and cell death was determined after 2 h or 4 h of treatment by LDH assay (\* $P$  < 0.05 vs. AA, # $P$  < 0.05 vs. PGD<sub>2</sub>). At least 3 independent experiments are shown.

to 100  $\mu$ M, neither arachidonic acid nor PGD<sub>2</sub> induced cell death in HSCs in contrast to NADA (Fig. 8E).

*GSH* levels also render hepatocytes resistant towards NADA-mediated death. Due to the fact that ROS formation is crucial for the cytotoxic effect of NADA in HSCs, we determined whether antioxidants are an additional mechanism for the resistance to NADA-induced cell death in hepatocytes. Previously, we (51) already showed that hepatocytes express GSH levels that are 10-fold higher than in HSCs. Accordingly, pretreatment with BSO rendered hepatocytes sensitive to NADA-induced cell death, leading to 28% cell death after treatment with 25  $\mu$ M NADA for 24 h (Fig. 7E). When hepatocytes were pretreated with a combination of BSO and URB597, NADA induced >50% cell death at a concentration of 50  $\mu$ M (Fig. 7E), and the threshold for NADA-induced cell death was lowered to 1  $\mu$ M (data not shown). Thus FAAH and GSH are main determinants of NADA-induced cell death in the liver.

## DISCUSSION

The capability to induce cell death in many different cell types has made endocannabinoids appealing targets for cancer, inflammatory, or degenerative diseases (16, 33). Knowledge

about the mechanisms that determine the susceptibility of primary cells toward the different types of endocannabinoid system may be helpful for therapeutic exploitation of the endocannabinoid system.

Recently, it has been demonstrated that the endocannabinoid system is involved in the regulation of fibrogenesis in the liver. CB2<sup>-/-</sup> mice showed increased fibrogenesis in response to CCl<sub>4</sub> injection, whereas CB1<sup>-/-</sup> mice had decreased hepatic fibrogenesis (26, 52). However, the mechanisms by which endocannabinoids regulate liver injury and fibrogenesis are not well characterized and require further investigation (49).

We have recently described that the endocannabinoids AEA or 2-AG selectively induce cell death in primary HSCs, the main fibrogenic cell type of the liver, but do not induce death in primary hepatocytes (48, 51). These actions occur independently of cannabinoid receptors but require membrane cholesterol. A selective induction of cell death in HSCs may contribute to the resolution of liver fibrosis, whereas hepatocyte cell death deteriorates liver function and promotes fibrogenesis (2). These properties suggest that modulation of the endocannabinoid system may be useful for the treatment of hepatic injury and fibrosis. However, it is yet unclear which endocannabi-

noids are responsible for the profibrotic signaling action of CB1 (52) or the antifibrotic effects of CB2 stimulation (26). In a recent study, Caraceni et al. (10) found a relevant increase in serum levels of the novel endocannabinoids oleyl ethanolamine and palmitoyl ethanolamine of human patients with liver cirrhosis, but the functional role of these endocannabinoids on cellular basis was not analyzed.

Here we demonstrate that the novel endocannabinoid NADA dose dependently induces death in activated primary HSCs, but not in hepatocytes, through an ROS-dependent mechanism independently from the cannabinoid receptors CB1 or CB2 or the vanilloid receptor TRPV1. Similar to HSC death induced by AEA, NADA rapidly and effectively caused necrotic cell death in HSCs starting at low micromolar concentrations. NADA-induced cell death appeared to be caspase 3-independent necrosis, since pan-caspase inhibition with Z-VAD-FMK only inhibited TNF- $\alpha$ -induced HSC apoptosis but not NADA-induced death.

Since endocannabinoids exhibit a volatile nature with short half-life due to their production on demand without storage capability and fast degradation (16), the rapid induction of cell death in primary HSCs by NADA shown *in vitro* implies a putative effective induction of death *in vivo*. NADA tissue levels *in vivo* were determined to be in comparable ranges as AEA in the rat striatum (24). Hepatic tissue levels of AEA as well as 2-AG have been shown to be significantly upregulated in the injured liver (25, 39, 48). AEA was determined to rise up to 2.0 nM (25), and 2-AG was even measured to be elevated up to 2.2  $\mu$ M (25, 48). We were able to detect NADA as well as AEA levels in the rat striatum also in the nanomolar range, which is consistent with previous reports (8, 23, 24). However, several groups were not able to detect NADA neither in the central nervous system (11, 30) nor in peripheral tissues or plasma (1, 53), indicating an extremely volatile and short-lived nature of this novel endocannabinoid. Accordingly, we were unable to measure NADA levels in livers from mice, rats, or humans. It might be possible that NADA is not produced in the liver under our conditions. Yet, we detected AEA levels in low nanomolar ranges in normal liver, and we found a significant, threefold increase in fibrotic liver, indicating the activation of the endocannabinoid system during liver injury and fibrogenesis. For interpretation of endocannabinoid levels *in vivo*, one has to keep in mind that endocannabinoids are produced instantly on demand and are rapidly degraded. Therefore, the detected endocannabinoid tissue concentrations might be significantly lower than the actual concentrations on the cellular level. At sites of proinflammatory cell activation, AEA levels could reach up to 50  $\mu$ M intracellularly (7). Thus it might be conceivable that concentrations of NADA may also quickly reach micromolar ranges on the cellular level that could exert antiproliferative or antifibrogenic actions or even rapidly induce cell death *in vivo*, since we were able to show that *in vivo*-activated HSCs were highly susceptible toward NADA and a very short exposure time was sufficient to effectively induce cell death in HSCs. However, further studies with exogenously applied NADA in models of murine liver fibrosis could corroborate the potential of NADA as an antifibrogenic tool.

When we tested the effects of sublethal concentrations of NADA on activated primary HSCs, we found a notable inhibitory effect on proliferation and migration, as shown in the

wound healing assay. To our knowledge, this is the first report on putative antiproliferative properties of NADA. This finding exceeds the antiproliferative properties of AEA, where we at least found an inhibition of DNA synthesis at concentrations between 1 and 10  $\mu$ M but not at nanomolar concentrations (51). When we examined the molecular mechanisms of the antiproliferative effect of NADA, we found an inhibition of ERK1/2 phosphorylation by NADA after addition of proproliferative FBS to serum-starved HSCs. ERK has been shown to be a kinase that mediates proliferative and antiapoptotic effects in myofibroblasts and HSCs (52). Moreover, NADA in sublethal concentrations was also able to slow down activation of freshly isolated primary mouse HSCs, which in contrast could not be achieved by comparable concentrations of AEA (51). This finding represents another aspect of the antifibrotic properties of NADA in the liver.

Concerning the pathways of NADA-induced cell death, previous studies reported NADA-mediated cell death through engagement of TRPV1 or CB2 receptors. One study (45) found NADA-induced death in human peripheral blood mononuclear cells that could be inhibited by pharmacological blockade of either TRPV1 or CB2 receptors. Whether NADA induced apoptotic or necrotic cell death was not analyzed. Another study (13) described a delayed form of cell death with apoptotic features in a neuronal cell line stably expressing recombinant human TRPV1. Untransfected cells of the same cell type were resistant against NADA. Although HSCs express all three putative cannabinoid or vanilloid receptors CB1, CB2, and TRPV1 (26, 51), we found a receptor-independent form of NADA-mediated necrotic cell death in HSCs, shown by pharmacologic and genetic approaches of receptor antagonism. We further tested, whether TRPV1 activation could generally induce HSC cell death. When we exposed HSCs to the specific TRPV1 agonist capsaicin, we did not observe any cell death even at concentrations up to 100  $\mu$ M. The differences of NADA-mediated type of cell death or dependence on CB2 or TRPV1 receptors might be due to different cell types, since we and others (26, 50, 51) have demonstrated earlier that endocannabinoids, *i.e.*, AEA or 2-AG, induce cell death in HSCs independently from CB1, CB2, or TRPV1. However, we also previously showed that AEA-mediated death occurred through interaction of AEA with membrane cholesterol. In contrast to AEA, NADA-induced HSC death could not be inhibited by membrane cholesterol depletion, indicating common downstream death signaling pathways of NADA and AEA but different upstream mechanisms. Cholesterol was shown to stimulate the insertion of AEA into, and its transport across lipid bilayer membranes, because AEA could adopt a shape that was remarkably complementary to cholesterol (18). This might not be the case for NADA. Recent studies (54) have suggested that endocannabinoids reach their site of action in cells through fast lateral diffusion across cell membrane bilayers. To do so, endocannabinoids such as AEA and 2-AG seem to require cholesterol, but NADA apparently does not.

Downstream mechanisms of NADA-induced death in HSCs comprise the rapid and substantial induction of ROS in similar ranges as AEA. ROS have previously been proposed as mediators of HSC activation and proliferation (4, 19). However, the proproliferative and activating effects of ROS in HSCs are mediated by low-level generation by membrane-bound NADPH oxidase. In contrast, our study detects high levels of rapid ROS

production after NADA treatment predominantly generated in the cytoplasm. High amounts of rapidly generated ROS are known to decrease cellular oxidative defense mechanisms, causing lipid peroxidation and leading to rapid damage of vitally important intracellular macromolecules, thus initiating necrosis (43). The fact that treatment of HSCs with antioxidants (GSH, Trolox) blocked and GSH depletion aggravated NADA-induced cell death underlines the pivotal role of ROS generation for HSC death induction. Moreover, ROS trigger the loss of cellular ATP by directly damaging mitochondrial DNA, enzymes such as ATP synthase, and cell organelle membranes (21, 43). We detected an early depletion of ATP in NADA-treated HSCs, one of the key characteristics of necrotic cell death (31, 34). ATP depletion causes inactivation of  $\text{Na}^+\text{-K}^+\text{-ATPase}$  entailing accumulation of intracellular  $\text{Na}^+$  and loss of  $\text{K}^+$ , accompanied by  $\text{Cl}^-$  increase and water influx with subsequent cell swelling and membrane blebbing (43), features that occur in HSCs after NADA treatment. To further analyze the signaling pathways leading to necrotic cell death by NADA in HSCs, we checked for the involvement of RIP1 as a key component of programmed necrosis/necroptosis. Programmed necrosis has been identified as a regulated mechanism of cell death when apoptosis is blocked and has been linked to ROS induction (56). However, inhibition of RIP1 did not inhibit NADA-mediated death, indicating that NADA does not induce necroptosis but pure necrosis. Other signaling pathways that are known to be affected by endocannabinoids and have concomitantly been related to cell death or survival of HSCs involving ROS are the JNK, NF- $\kappa$ B (51), and AKT (40) pathways. NADA led to JNK activation, which, however, did not causatively contribute to NADA-induced cell death. In contrast to AEA, NADA neither activated nor inhibited NF- $\kappa$ B activation. Finally, NADA phosphorylated AKT, but this protective pathway could not inhibit NADA-induced cell death. Thus NADA cell death signaling in HSCs appears to depend on excessive ROS production with subsequent initiation of intracellular damage and ATP depletion without requirement of JNK activation, or inhibition of NF- $\kappa$ B or AKT, respectively.

The induction of cell death in HSCs by NADA was highly effective compared with other lipid mediators. We compared NADA to its precursor/metabolite arachidonic acid (23) and the arachidonic acid derivative  $\text{PGD}_2$ , which plays an important role in COX-2-mediated degradation of endocannabinoids (29). All substances feature polyunsaturated acyl chains that might induce cell death because of detergent-like perturbation of the cell membrane and increased ROS formation followed by lipid peroxidation (42). The significantly higher rate of cell death by NADA even when we applied excessive concentrations of the control substances up to 100  $\mu\text{M}$  might be due to structural differences between these substances leading to lower binding of arachidonic acid or  $\text{PGD}_2$  to HSCs with subsequently lower toxicity.

In our initial analysis of expression of the rate-limiting NADA-generating enzyme TH (24), we found a stable expression pattern in normal as well as in fibrotic liver. Strikingly, TH was mainly expressed in sympathetic neurons that run along the portal tracts, suggesting that this neural tissue might be the putative main source of NADA in the liver. Hepatocytes express TH on mRNA and protein levels but to a significantly lower level than sympathetic neural tissue. Nonparenchymal cells such as HSCs, Kupffer cells or LSECs only express

scarce traces of the enzyme. Therefore, in contrast to NADA degradation, neither hepatocytes nor nonparenchymal cell populations seem to be critically involved in the generation of NADA in the liver.

Interestingly, hepatocytes were largely resistant against cell death induced by NADA in contrast to HSCs. This remarkable resistance of hepatocytes against NADA death was due to the effective antioxidant defense mechanism of high GSH expression. However, in pathological conditions such as advanced liver cirrhosis or alcoholic liver disease, hepatic antioxidant defense mechanisms, e.g., GSH levels, are severely diminished (2). The reduction of antioxidants could render hepatocytes highly susceptible toward the deleterious effects of oxidative lipid mediators such as polyunsaturated free fatty acids or endocannabinoids. Due to the fact that antioxidant levels confer only partial resistance against NADA in hepatocytes and could be significantly depleted *in vivo*, we analyzed additional factors that caused hepatocyte resistance against NADA-induced death. Methylation represents one mechanism for the partial inactivation of NADA (24). NADA is converted by catechol-o-methyl-transferase (COMT) to its less potent 3-*O*-methyl derivative. However, COMT expression was neither significantly detectable in hepatocytes nor in HSCs. Consequently, this degradation pathway did not contribute to the NADA resistance of hepatocytes, since selective pharmacological inhibition of COMT did not render hepatocytes susceptible toward NADA death. Another more effective degradation pathway of NADA is its hydrolyzation by FAAH into arachidonic acid and dopamine (23, 24). FAAH has initially been identified as the primary degradation enzyme for AEA (12). FAAH is highly expressed in hepatocytes but not in HSCs and has been shown by our group to play a pivotal role in the resistance of hepatocytes against AEA-induced cell death (50). When we inhibited FAAH with the selective FAAH inhibitor URB597, we were able to make hepatocytes susceptible toward NADA and in addition, FAAH<sup>-/-</sup> hepatocytes displayed a high vulnerability for NADA. Thus like AEA, NADA does not induce cell death in hepatocytes unless they are severely depleted of GSH or FAAH has been inactivated. As a proof of principle, adenoviral overexpression of FAAH in HSCs conferred resistance against NADA, underlining the pivotal role of FAAH in the resistance of liver cell populations against NADA. These crucial protective properties of FAAH against endocannabinoids possibly apply also to pathological liver conditions that are accompanied by reduced antioxidant defense levels. Another evidence of the importance of FAAH in NADA resistance was the fact that the hydrolyzation products arachidonic acid and dopamine did not induce cell death in HSCs. However, it has been shown that AEA was a better substrate for FAAH than NADA (23, 24), possibly explaining the slightly higher resistance of hepatocytes against AEA- than NADA-induced cell death. FAAH was also shown to be a putative synthesizing enzyme for NADA (23), but since FAAH primarily conferred cellular resistance against NADA-induced cell death, we assume rather an essential role for FAAH in NADA degradation in these liver cell populations than in NADA synthesis.

In conclusion, the selective expression of effective defense systems (antioxidants and FAAH) in hepatocytes as well as the selective and efficient induction of cell death in HSCs and its

inhibitory effects on HSC activation and proliferation propose NADA as a novel antifibrotic agent.

#### ACKNOWLEDGMENTS

We thank Bruno Pradier (Institute of Molecular Psychiatry, University of Bonn) for excellent assistance in the preparation of dorsal root ganglia and Claudia Schwitter (Institute of Physiological Chemistry, University Medical Center Mainz) for outstanding help with the endocannabinoid measurements.

#### GRANTS

The study was supported by Deutsche Forschungsgemeinschaft Grants S1 1366/1-1 and SFB TRR57 Project 15 (to S. V. Siegmund), SFB TRR57 Project Q1 to (S. Huss), SFB TRR57 Project P11 (to P. A. Knolle), SFB TRR57 Project 18 (to J. Trebicka and T. Sauerbruch), FOR926 (to B. Lutz), and FOR926 and SFB TRR57 Project 15 (to A. Zimmer).

#### DISCLOSURES

No conflicts of interest, financial or otherwise, are declared by the author(s).

#### AUTHOR CONTRIBUTIONS

Author contributions: A.W., F.H., M.G., S.K., J.T., S.H., R.L., F.A.S., P.A.K., and S.V.S. performed experiments; A.W., F.H., M.G., S.K., J.T., S.H., R.L., B.L., F.A.S., P.A.K., A.Z., and S.V.S. analyzed data; A.W., F.H., M.G., S.K., J.T., S.H., R.L., B.L., F.A.S., P.A.K., T.S., M.V.S., A.Z., and S.V.S. interpreted results of experiments; A.W., F.H., M.G., S.H., and S.V.S. prepared figures; A.W. and S.V.S. drafted manuscript; A.W., F.H., M.G., S.K., J.T., S.H., R.L., B.L., F.A.S., P.A.K., T.S., M.V.S., A.Z., and S.V.S. approved final version of manuscript; J.T., B.L., T.S., M.V.S., A.Z., and S.V.S. edited and revised manuscript; S.V.S. conception and design of research.

#### REFERENCES

- Balvers MG, Verhoeckx KC, Witkamp RF. Development and validation of a quantitative method for the determination of 12 endocannabinoids and related compounds in human plasma using liquid chromatography-tandem mass spectrometry. *J Chromatogr B Analyt Technol Biomed Life Sci* 877: 1583–1590, 2009.
- Bataller R, Brenner DA. Liver fibrosis. *J Clin Invest* 115: 209–218, 2005.
- Bataller R, Gabele E, Parsons CJ, Morris T, Yang L, Schoonhoven R, Brenner DA, Rippe RA. Systemic infusion of angiotensin II exacerbates liver fibrosis in bile duct-ligated rats. *Hepatology* 41: 1046–1055, 2005.
- Bataller R, Schwabe RF, Choi YH, Yang L, Paik YH, Lindquist J, Qian T, Schoonhoven R, Hagedorn CH, Lemasters JJ, Brenner DA. NADPH oxidase signal transduces angiotensin II in hepatic stellate cells and is critical in hepatic fibrosis. *J Clin Invest* 112: 1383–1394, 2003.
- Begg M, Pacher P, Batkai S, Osei-Hyiaman D, Offertaler L, Mo FM, Liu J, Kunos G. Evidence for novel cannabinoid receptors. *Pharmacol Ther* 106: 133–145, 2005.
- Bisogno T, Melck B, Bobrov M, Gretskey NM, Bezuglov VV, De Petrocellis L, Di Marzo V. N-acyl-dopamines: novel synthetic CB(1) cannabinoid-receptor ligands and inhibitors of anandamide inactivation with cannabimimetic activity in vitro and in vivo. *Biochem J* 351: 817–824, 2000.
- Biswas KK, Sarker KP, Abeyama K, Kawahara K, Iino S, Otsubo Y, Saigo K, Izumi H, Hashiguchi T, Yamakuchi M, Yamaji K, Endo R, Suzuki K, Imaizumi H, Maruyama I. Membrane cholesterol but not putative receptors mediates anandamide-induced hepatocyte apoptosis. *Hepatology* 38: 1167–1177, 2003.
- Bradshaw HB, Rimmerman N, Krey JF, Walker JM. Sex and hormonal cycle differences in rat brain levels of pain-related cannabimimetic lipid mediators. *Am J Physiol Regul Integr Comp Physiol* 291: R349–R358, 2006.
- Brumovsky P, Villar MJ, Hokfelt T. Tyrosine hydroxylase is expressed in a subpopulation of small dorsal root ganglion neurons in the adult mouse. *Exp Neurol* 200: 153–165, 2006.
- Caraceni P, Viola A, Piscitelli F, Giannone F, Berzigotti A, Cescon M, Domenicali M, Petrosino S, Giampalma E, Riili A, Grazi G, Golfieri R, Zoli M, Bernardi M, Di Marzo V. Circulating and hepatic endocannabinoids and endocannabinoid-related molecules in patients with cirrhosis. *Liver Int* 30: 816–825, 2010.
- Chen J, Paudel KS, Derbenev AV, Smith BN, Stinchcomb AL. Simultaneous quantification of anandamide and other endocannabinoids in dorsal vagal complex of rat brainstem by LC-MS. *Chromatographia* 69: 1–7, 2009.
- Cravatt BF, Giang DK, Mayfield SP, Boger DL, Lerner RA, Gilula NB. Molecular characterization of an enzyme that degrades neuromodulatory fatty-acid amides. *Nature* 384: 83–87, 1996.
- Davies JW, Hainsworth AH, Guerin CJ, Lambert DG. Pharmacology of capsaicin-, anandamide-, and N-arachidonoyl-dopamine-evoked cell death in a homogeneous transient receptor potential vanilloid subtype 1 receptor population. *Br J Anaesth* 104: 596–602, 2010.
- De Minicis S, Seki E, Uchinami H, Kluwe J, Zhang Y, Brenner DA, Schwabe RF. Gene expression profiles during hepatic stellate cell activation in culture and in vivo. *Gastroenterology* 132: 1937–1946, 2007.
- Devane WA, Hanus L, Breuer A, Pertwee RG, Stevenson LA, Griffin G, Gibson D, Mandelbaum A, Etinger A, Mechoulam R. Isolation and structure of a brain constituent that binds to the cannabinoid receptor. *Science* 258: 1946–1949, 1992.
- Di Marzo V, Bifulco M, De Petrocellis L. The endocannabinoid system and its therapeutic exploitation. *Nat Rev Drug Discov* 3: 771–784, 2004.
- Di Marzo V, Matias I. Endocannabinoid control of food intake and energy balance. *Nat Neurosci* 8: 585–589, 2005.
- Di Pasquale E, Chahinian H, Sanchez P, Fantini J. The insertion and transport of anandamide in synthetic lipid membranes are both cholesterol-dependent. *PLoS One* 4: e4989, 2009.
- Galli A, Svegliati-Baroni G, Ceni E, Milani S, Ridolfi F, Salzano R, Tarocchi M, Grappone C, Pellegrini G, Benedetti A, Surrenti C, Casini A. Oxidative stress stimulates proliferation and invasiveness of hepatic stellate cells via a MMP2-mediated mechanism. *Hepatology* 41: 1074–1084, 2005.
- Harrison S, De Petrocellis L, Trevisani M, Benvenuti F, Bifulco M, Geppetti P, Di Marzo V. Capsaicin-like effects of N-arachidonoyl-dopamine in the isolated guinea pig bronchi and urinary bladder. *Eur J Pharmacol* 475: 107–114, 2003.
- Hoek JB, Cahill A, Pastorino JG. Alcohol and mitochondria: a dysfunctional relationship. *Gastroenterology* 122: 2049–2063, 2002.
- Hoyer FF, Steinmetz M, Zimmer S, Becker A, Lutjohann D, Buchalla R, Zimmer A, Nickenig G. Atheroprotection via cannabinoid receptor-2 is mediated by circulating and vascular cells in vivo. *J Mol Cell Cardiol* 51: 1007–1014, 2011.
- Hu SS, Bradshaw HB, Benton VM, Chen JS, Huang SM, Minassi A, Bisogno T, Masuda K, Tan B, Roskoski R Jr, Cravatt BF, Di Marzo V, Walker JM. The biosynthesis of N-arachidonoyl dopamine (NADA), a putative endocannabinoid and endovanilloid, via conjugation of arachidonic acid with dopamine. *Prostaglandins Leukot Essent Fatty Acids* 81: 291–301, 2009.
- Huang SM, Bisogno T, Trevisani M, Al-Hayani A, De Petrocellis L, Fezza F, Tognetto M, Petros TJ, Krey JF, Chu CJ, Miller JD, Davies SN, Geppetti P, Walker JM, Di Marzo V. An endogenous capsaicin-like substance with high potency at recombinant and native vanilloid VR1 receptors. *Proc Natl Acad Sci USA* 99: 8400–8405, 2002.
- Jeong WI, Osei-Hyiaman D, Park O, Liu J, Batkai S, Mukhopadhyay P, Horiguchi N, Harvey-White J, Marsicano G, Lutz B, Gao B, Kunos G. Paracrine activation of hepatic CB1 receptors by stellate cell-derived endocannabinoids mediates alcoholic fatty liver. *Cell Metab* 7: 227–235, 2008.
- Julien B, Grenard P, Teixeira-Clerc F, Van Nhieu JT, Li L, Karsak M, Zimmer A, Mallat A, Lotersztajn S. Antifibrogenic role of the cannabinoid receptor CB2 in the liver. *Gastroenterology* 128: 742–755, 2005.
- Kathuria S, Gaetani S, Fegley D, Valino F, Duranti A, Tontini A, Mor M, Tarzia G, La Rana G, Calignano A, Giustino A, Tattoli M, Palmery M, Cuomo V, Piomelli D. Modulation of anxiety through blockade of anandamide hydrolysis. *Nat Med* 9: 76–81, 2003.
- Klein TW. Cannabinoid-based drugs as anti-inflammatory therapeutics. *Nat Rev Immunol* 5: 400–411, 2005.
- Kozak KR, Rowlinson SW, Marnett LJ. Oxygenation of the endocannabinoid, 2-arachidonoylglycerol, to glyceryl prostaglandins by cyclooxygenase-2. *J Biol Chem* 275: 33744–33749, 2000.
- Lehtonen M, Storvik M, Malinen H, Hyytia P, Lakso M, Auriola S, Wong G, Callaway JC. Determination of endocannabinoids in nematodes and human brain tissue by liquid chromatography electrospray ionization tandem mass spectrometry. *J Chromatogr B Analyt Technol Biomed Life Sci* 879: 677–694.

31. Lemasters JJV. Necroptosis and the mitochondrial permeability transition: shared pathways to necrosis and apoptosis. *Am J Physiol Gastrointest Liver Physiol* 276: G1–G6, 1999.
32. Lim MP, Devi LA, Rozenfeld R. Cannabidiol causes activated hepatic stellate cell death through a mechanism of endoplasmic reticulum stress-induced apoptosis. *Cell Death Dis* 2: e170, 2011.
33. Maccarrone M, Finazzi-Agro A. The endocannabinoid system, anandamide and the regulation of mammalian cell apoptosis. *Cell Death Differ* 10: 946–955, 2003.
34. Malhi H, Gores GJ, Lemasters JJ. Apoptosis and necrosis in the liver: a tale of two deaths? *Hepatology* 43: S31–S44, 2006.
35. Movsesyan VA, Stoica BA, Yakovlev AG, Knoblach SM, Lea PM, Cernak I, Vink R, Faden AI. Anandamide-induced cell death in primary neuronal cultures: role of calpain and caspase pathways. *Cell Death Differ* 11: 1121–1132, 2004.
36. Munro S, Thomas KL, Abu-Shaar M. Molecular characterization of a peripheral receptor for cannabinoids. *Nature* 365: 61–65, 1993.
37. O'Sullivan SE, Kendall DA, Randall MD. Characterisation of the vasorelaxant properties of the novel endocannabinoid N-arachidonoyl-dopamine (NADA). *Br J Pharmacol* 141: 803–812, 2004.
38. O'Sullivan SE, Kendall DA, Randall MD. Vascular effects of delta 9-tetrahydrocannabinol (THC), anandamide and N-arachidonoyldopamine (NADA) in the rat isolated aorta. *Eur J Pharmacol* 507: 211–221, 2005.
39. Osei-Hyiaman D, DePetrillo M, Pacher P, Liu J, Radaeva S, Batkai S, Harvey-White J, Mackie K, Offertaler L, Wang L, Kunos G. Endocannabinoid activation at hepatic CB1 receptors stimulates fatty acid synthesis and contributes to diet-induced obesity. *J Clin Invest* 115: 1298–1305, 2005.
40. Perez de Obanos MP, Lopez-Zabalza MJ, Arriazu E, Modol T, Prieto J, Herraiz MT, Iraburu MJ. Reactive oxygen species (ROS) mediate the effects of leucine on translation regulation and type I collagen production in hepatic stellate cells. *Biochim Biophys Acta* 1773: 1681–1688, 2007.
41. Pinzani M, Marra F. Cytokine receptors and signaling in hepatic stellate cells. *Semin Liver Dis* 21: 397–416, 2001.
42. Pompeia C, Lima T, Curi R. Arachidonic acid cytotoxicity: can arachidonic acid be a physiological mediator of cell death? *Cell Biochem Funct* 21: 97–104, 2003.
43. Raffray M, Cohen GM. Apoptosis and necrosis in toxicology: a continuum or distinct modes of cell death? *Pharmacol Ther* 75: 153–177, 1997.
44. Sarker KP, Maruyama I. Anandamide induces cell death independently of cannabinoid receptors or vanilloid receptor 1: possible involvement of lipid rafts. *Cell Mol Life Sci* 60: 1200–1208, 2003.
45. Saunders CI, Fassett RG, Geraghty DP. Up-regulation of TRPV1 in mononuclear cells of end-stage kidney disease patients increases susceptibility to N-arachidonoyl-dopamine (NADA)-induced cell death. *Biochim Biophys Acta* 1792: 1019–1026, 2009.
46. Schurich A, Berg M, Stabenow D, Bottcher J, Kern M, Schild HJ, Kurts C, Schuette V, Burgdorf S, Diehl L, Limmer A, Knolle PA. Dynamic regulation of CD8 T cell tolerance induction by liver sinusoidal endothelial cells. *J Immunol* 184: 4107–4114, 2010.
47. Seki E, De Minicis S, Osterreicher CH, Kluwe J, Osawa Y, Brenner DA, Schwabe RF. TLR4 enhances TGF-beta signaling and hepatic fibrosis. *Nat Med* 13: 1324–1332, 2007.
48. Siegmund SV, Qian T, de Minicis S, Harvey-White J, Kunos G, Vinod KY, Hungund B, Schwabe RF. The endocannabinoid 2-arachidonoyl glycerol induces death of hepatic stellate cells via mitochondrial reactive oxygen species. *FASEB J* 21: 2798–2806, 2007.
49. Siegmund SV, Schwabe RF. Endocannabinoids and liver disease. II. Endocannabinoids in the pathogenesis and treatment of liver fibrosis. *Am J Physiol Gastrointest Liver Physiol* 294: G357–G362, 2008.
50. Siegmund SV, Seki E, Osawa Y, Uchinami H, Cravatt BF, Schwabe RF. Fatty acid amide hydrolase determines anandamide-induced cell death in the liver. *J Biol Chem* 281: 10431–10438, 2006.
51. Siegmund SV, Uchinami H, Osawa Y, Brenner DA, Schwabe RF. Anandamide induces necrosis in primary hepatic stellate cells. *Hepatology* 41: 1085–1095, 2005.
52. Teixeira-Clerc F, Julien B, Grenard P, Tran Van Nhieu J, Deveaux V, Li L, Serriere-Lanneau V, Ledent C, Mallat A, Lotersztajn S. CB1 cannabinoid receptor antagonism: a new strategy for the treatment of liver fibrosis. *Nat Med* 12: 671–676, 2006.
53. Thomas A, Hopfgartner G, Giroud C, Staub C. Quantitative and qualitative profiling of endocannabinoids in human plasma using a triple quadrupole linear ion trap mass spectrometer with liquid chromatography. *Rapid Commun Mass Spectrom* 23: 629–638, 2009.
54. Tian X, Guo J, Yao F, Yang DP, Makriyannis A. The conformation, location, and dynamic properties of the endocannabinoid ligand anandamide in a membrane bilayer. *J Biol Chem* 280: 29788–29795, 2005.
55. Trebicka J, Racz I, Siegmund SV, Cara E, Granzow M, Schierwagen R, Klein S, Wojtalla A, Hennenberg M, Huss S, Fischer HP, Heller J, Zimmer A, Sauerbruch T. Role of cannabinoid receptors in alcoholic hepatic injury: steatosis and fibrogenesis are increased in CB(2) receptor-deficient mice and decreased in CB(1) receptor knockouts. *Liver Int* 31: 862–872.
56. Vandebeele P, Galluzzi L, Vanden Berghe T, Kroemer G. Molecular mechanisms of necroptosis: an ordered cellular explosion. *Nat Rev Mol Cell Biol* 11: 700–714.